Olivine-Rich Submarine Basalts From the Southwest Rift Zone of Mauna Loa Volcano: Implications for Magmatic Processes and Geochemical Evolution

Michael O. Garcia, Thomas P. Hulsebosch

Department of Geology & Geophysics, University of Hawaii, Honolulu, Hawaii

J. Michael Rhodes

University of Massachusetts, Amherst, Massachusetts

The east Ka Lae landslide on the submarine south flank of Mauna Loa exposed a 1.3 km thick section into the interior of its southwest rift zone. We sampled this section in four dredge hauls and four submersible dives and made a multibeam survey of the rift zone. New magnetic data and our observations and bathymetric results indicate that the axis of the southwest rift is two to three kilometers west of the present topographic high. Our submersible observations of old beach deposits and the low sulfur content of pillow-rim glasses indicate that this portion of the southwest rift zone has subsided >400 m. Olivine-rich basalts are extremely abundant along the submarine portion of Mauna Loa's southwest rift zone but their abundance decreases significantly in the upper parts of the two sections examined. This change probably occurred ~ 60 ka when Mauna Loa's eruption rate slowed and was unable to keep up with its subsidence rate. The dense magmas for these olivine-rich basalts were probably intruded into the deeper portions of the rift zones and erupted from its distal regions during periods of high magma supply. The preferential eruption of olivine-rich lavas on the flanks of Mauna Loa and other Hawaiian volcanoes is a strong indication that a density filter operates within these volcanoes. These lavas contain abundant euhedral, undeformed olivine with high forsterite contents (typically 90%). Some of these olivines grew in magmas with 17.5 wt% MgO at temperatures of 1415°C, indicating that Hawaiian tholeiitic magmas are some of the most mafic and hottest magmas erupted during the Cenozoic. All of the submarine lavas have major element contents typical of Mauna Loa, but unlike its subaerial lavas, some of the submarine lavas have trace element and isotope ratios that overlap with those of Kilauea lavas. Thus, the source for Mauna Loa contained a Kilauea-like component that has been consumed during the last hundred thousand years, but the melt extraction conditions that have controlled the major elements in Mauna Loa lavas has remained relatively constant.

INTRODUCTION

Mauna Loa is the largest volcano on Earth. It stands ~8.5 km above the seafloor and has a keel under the summit of the volcano that extends about 5 km below the seafloor [*Hill and Zucca, 1987*]. The volume of Mauna Loa above the sea floor has been estimated at ~42,000 km^3 [*Bargar and Jackson, 1974*]. *Lipman* [*this volume*] suggests that the Bargar and *Jackson* [*1974*] volume estimate is too low by 23,000 km^3 because the size of the adjacent volcano, Kilauea, was overestimated. Our estimate for the keel volume is ~40,000 km^3 based on limited seismic refraction data [*Hill and Zucca, 1987*]. This agrees with *Moore's* [*1987*] suggestion that ~50% of the volume of Hawaiian volcanoes is beneath the level of the sea floor. Thus, Mauna Loa may have a total volume of ~105,000 km^3. *Lipman* [*this volume*] estimates the volcano's volume at ~80,000 km^3. The differences in these volumes are probably within the uncertainties of our estimates for the locations of the volcano's base and it boundaries with its three neighbor volcanoes.

Mauna Loa Revealed: Structure,
Composition, History, and Hazards
Geophysical Monograph 92

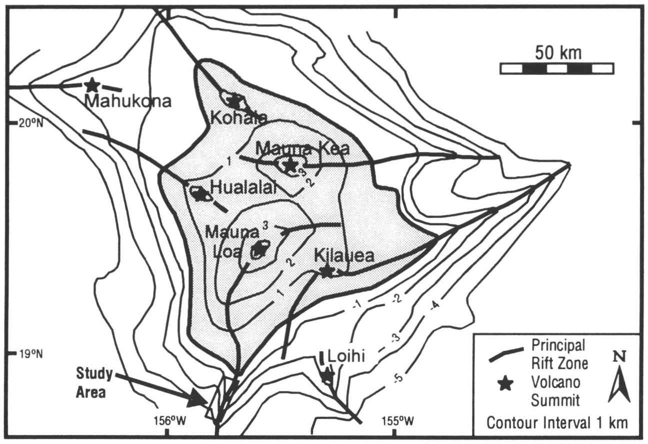

Fig. 1. Topographic map of the island of Hawaii showing the location of the summit and rift zones for the seven volcanoes that comprise the island [after *Lonsdale, 1989*].

The submarine portion of Mauna Loa Volcano has received limited geologic study because a detailed bathymetric map was not available until recently [*Chadwick et al., 1993; Moore and Chadwick, this volume*]. The previous studies of submarine Mauna Loa have focused on its shallow portions in order to examine the growth rate and subsidence history of the volcano [*Moore and Clague, 1987; Moore et al., 1990*]; features from the 1877 submarine eruption [*Fornari et al., 1980*]; and the morphology of the southwest rift zone [*Fornari et al., 1979*]. The giant landslides on the submarine flanks of Mauna Loa were examined by *Lipman et al.* [*1988*], *Moore et al.* [*1989*], and *Moore et al.* [*1995*]. Two reconnaissance dredging programs along the southwest rift zone recovered basalts that were included in broader studies of the submarine lavas of Hawaiian volcanoes [*Moore, 1966; Garcia et al., 1989*]. In contrast, the subaerial portion of the volcano is relatively well studied as a result of past and current geologic mapping by U.S. Geological Survey [*e.g., Lipman and Swenson, 1984; Lockwood et al., 1988*] and geochemical studies [*e.g., Wright, 1971; Rhodes, 1983; 1988; Kurz and Kammer, 1991; Rhodes and Hart, this volume*].

This study focused on the intermediate-depth portion of Mauna Loa's submarine south west rift zone (550-2000 m below sea level; mbsl). We present here the results of a new Seabeam survey along the rift zone and our petrographic, glass, and mineral chemistry studies of lavas collected from four submersible dives and four dredge hauls on the deeply dissected west flank of the rift zone. Our results show that Mauna Loa's submarine flanks are dominated by olivine-rich basalts. These basalts contain high forsterite olivine phenocrysts (up to 91.3% forsterite; Fo) which grew in magmas with up to 17.5 wt% MgO. The major element contents of glasses from these basalts are identical to modern Mauna Loa lavas, indicating that there has been little or no change in the volcano's partial melting processes for perhaps a few hundred thousand years. Some of these rocks, however, have distinct trace element ratios that require a different source, one geochemically similar to that which is currently supplying Kilauea Volcano. This source component was apparently exhausted during the last hundred thousand years and may have had a lower melting temperature.

Geologic Setting

Mauna Loa has two prominent rift zones, one trending northeast and the other southwest (Figure 1). The southwest rift zone extends ~65 km subaerially and ~35 km below sea level to a depth of ~5000 m. It has >8 km of relief along which it erupts lava. There is a distinct bend in the rift about 2400 m above sea level where its trend becomes southward. Below this bend, the rift is marked by the Kahuku scarp. The subaerial portion of this scarp has up to 200 m of relief and is buried up rift by younger lavas. The submarine extension of the Kahuku scarp has up to 1800 m of relief. Unlike other subaerial scarps on Mauna Loa and its neighbor Kilauea, the Kahuku scarp is not draped by younger lavas [*Fornari et al., 1979; Moore et al., 1990*]. Thus, although Mauna Loa is still active (the most recent eruption was in 1984), apparently little Holocene volcanic activity has occurred along the submarine portion of the rift. This makes this portion of the Kahuku scarp a superb area to sample the deepest exposures of Mauna Loa's interior, and it provides the best available opportunity to evaluate the long-term magmatic history of the volcano.

The ages of the lavas in the submarine section of Mauna Loa's southwest rift are poorly known. The thickness of the section (~1.3 km) and its distance from the summit (where volcanic activity is more frequent; *Lockwood and Lipman, 1987*) indicate that the submarine section probably contains lavas older than the oldest exposed subaerial lavas on Mauna Loa (the 100 to 200 ka Ninole basalts; *Lipman et al., 1990*). Attempts to date the submarine lavas were unsuccessful because of the low radiogenic argon content of the lavas. The ages obtained range from 0.12 to 1.5 Ma with no correlation with stratigraphic position [*Lipman, this volume*]. Our best estimate for the age of the submarine lavas is 100 to 300 ka based on extrapolation of the subaerial lava ages. *Lipman's* [*this volume*] estimate is 200-350 ka.

Sampling and Geological Observations

Four dredge hauls were made on Mauna Loa (Figure 2) during a 1982 R/V Kana Keoki cruise to sample the submarine rifts of all the volcanoes that form the island of Hawaii.

These dredge hauls were made up the steep western face of the southwest rift zone at depths between 1650-2600 mbsl for hauls 1, 2, and 4 and 1000-2200 mbsl for dredge haul 3. A variety of petrographically distinct rocks was recovered from each dredge haul. A representative sample of each distinct rock type from each dredge haul was selected for petrographic and geochemical analysis. The petrography, glass, and volatile chemistry of these samples was presented by *Garcia et al.* [*1989*]. Whole-rock analyses for some of these lavas were reported by *Gurriet* [*1988*]. These samples are coded ML followed by the dredge haul and sample numbers.

Our 1991 submersible sampling program was designed to collect from two sections up the face of the Kahuku scarp and to sample along the topographic axis of the rift zone (Figure 2). We used the Hawaii Undersea Research Lab's Pisces V submersible which has a depth limit of 2000 m. Three dives up the scarp (numbered 182-184) produced 36 samples collected in situ from Mauna Loa's thickest stratigraphic section (~1.3 km; the thickest subaerial section is ~600 m; *Lipman et al., 1990*). Eleven samples were collected during dive 185 along the crest of the ridge between 1505 and 1825 mbsl. Samples were collected from depths about 20 to 30 m apart whenever possible. Each sample was treated as a separate flow unit. One dike was sampled.

The geologic features we observed from the submersible's portholes and from reviewing the videotapes taken during the dives are summarized in Figure 3. Dive 182 started on a flat bench just west of the cliff face at a depth of 1870 mbsl. The steep face started at ~1800 mbsl. The base of the cliff is mantled to a depth of 1430 mbsl with mostly columnar-jointed talus derived from dikes in the cliff face [*as noted by Fornari et al., 1979*]. Above 1430 mbsl, outcrops of pillow lavas are abundant in near-vertical faces with intervening areas of moderately sloping talus. The pillow lavas are cut locally by numerous, steeply dipping dikes, which appear to be buttressing the steep cliffs (45° to vertical). The dikes are 1 to 3 m wide and trend roughly north-south. Dive 183 continued the traverse up the steep face of the ridge starting at 1200 mbsl (where dive 182 ended) and ending at 40 mbsl. We observed more pillow lavas cut by dikes during this dive, except at 425 mbsl where boulders and carbonate sand were encountered, and at 165-190 mbsl where a dead coral reef was found (Figure 3). The shallowest pillow lavas were observed at 300 mbsl.

Dive 184 started about 3.5 km south of the area traversed during dives 182 and 183, beginning at a depth of 1790 mbsl and ascending to the ridge crest at 550 mbsl. On this traverse we found the same features noted in dives 182 and 183, except that 0.5 to 1 m thick tephra layers were found at 745 and 775 mbsl interbedded with pillow lavas, and no boulders or coral were observed. The top of the ridge at this location is a bench underlain by a ~ 30 m thick massive flow. Pillow lavas were collected during this dive from 1790 to 550 mbsl.

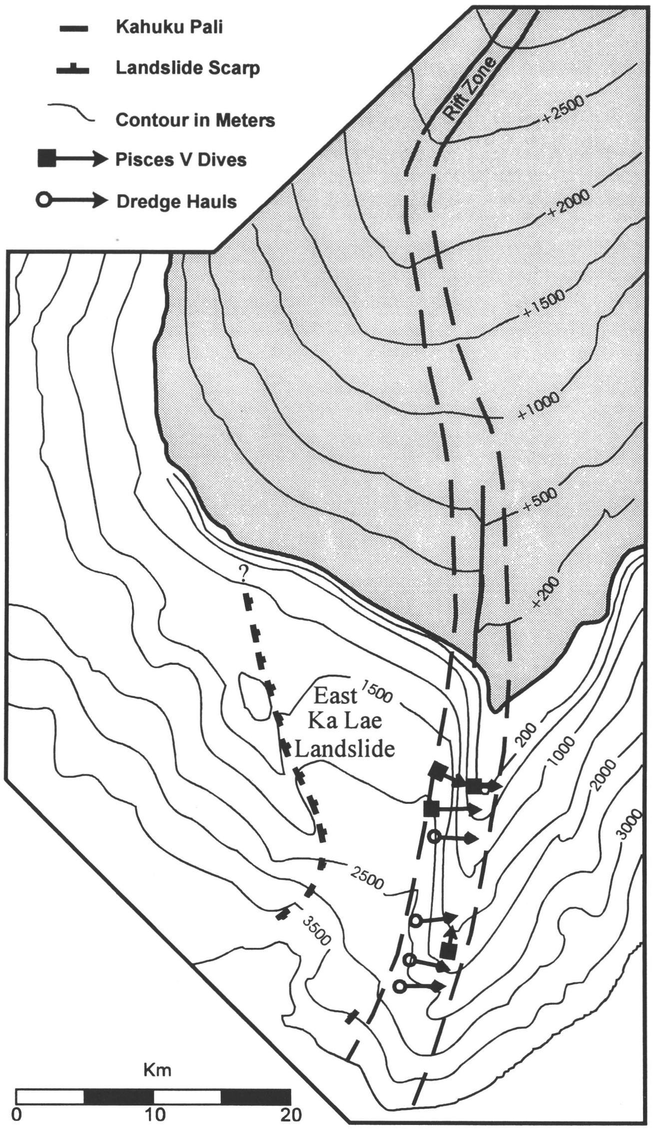

Fig. 2. Generalized topographic map of the lower portion of the southwest rift zone [after *Chadwick et al, 1993*] showing the location of dredge hauls, Pisces V dives, the Kahuku Fault, and the east Ka Lae landslide (boundaries shown by strike and dip symbols). Dashed parallel lines show the proposed location of Mauna Loa's southwest rift zone.

Dive 185 was along the crest of the ridge between 1825 and 1500 mbsl. The crest consisted of moderately dipping (10-20°) segments with rare pillow cones, separated by cliffs. No signs of recent volcanic or hydrothermal activity were observed.

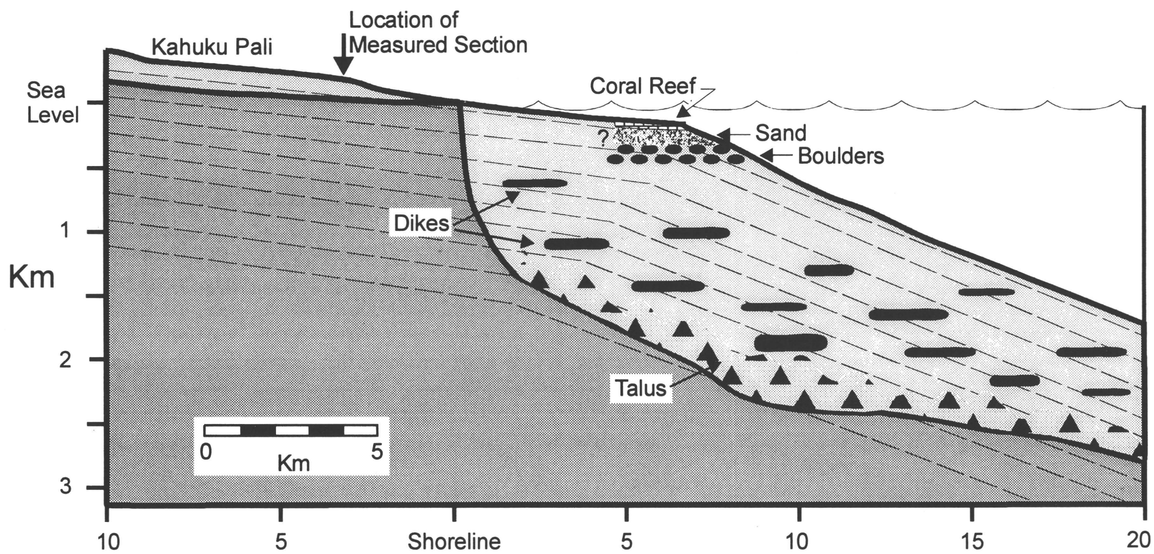

Fig. 3. Diagrammatic representation of the geology of the cliff face along the southwest rift zone (light gray area) based on observations from submersible dives. The dip of the lavas (dashed lines) increases just south of the dead coral reef, reflecting the steep submarine slope of Hawaiian volcanoes. Note the old shoreline deposits (sand and rounded boulders) below the reef. Dikes (black bands) are common to abundant in the cliff face; they trend nearly parallel to the cliff face and outcrop as walls. Vertical exaggeration is about 4x.

BATHYMETRY

The bathymetry of Mauna Loa's southwest rift was not well known prior to our study. Single-beam profiles had been made of the rift [*Fornari et al., 1979; Moore et al., 1990*] and a general (100 m contour) bathymetric map was constructed by *Moore et al.* [*1990*]. A more detailed map by *Moore and Clague* [*1992*] combined multibeam surveys west of the rift zone (longitude 155°45') with single-beam surveys across the rift. We had the opportunity in 1992 to make a multibeam survey of the rift zone with the U. S. Navy ship Laney Chouset. This new bathymetric map (Plate 1) combines our results with those of two previous NOAA multibeam surveys on either side of the rift. Our survey coverage is virtually continuous on the flanks of the rift and below 1200 mbsl. The coverage is 50-75% for depths between 500 -1200 mbsl and <50% above 500 mbsl along the rift.

The most striking feature of the new bathymetric map is the steep scarp along the west flank of the rift zone (Plate 1). This scarp extends onshore, where it is known as the Kahuku pali and only has ~10% of the relief of the submarine scarp. This scarp may have been created by the east Ka Lae landslide, rather than by faulting as proposed by *Lipman and Swenson* [*1984*] (Figure 2). The landslide is thought to have formed in one catastrophic event [*Moore et al., 1989*]. The smaller subaerial expression of the scarp may be a result of subsequent subaerial volcanism. The western detachment surface of the landslide may be defined by a prominent ridge, which was interpreted by *Lipman* [*1980*] to be a down-dropped block similar to those on the south flank of Kilauea. In the new bathymetry, however, there is no obvious bathymetric expression of the block slumping. We interpret the ridge as an erosional remnant of the landslide. The base of the slide may have several steps at 1300-1550, 2050-2400, and 2480-2590 mbsl (Plate 1). Down slope from the deepest step there is a debris chute that turns to the south at 4200 mbsl.

Another significant feature on Plate 1 is the continuation of the subaerial slope of Mauna Loa on its south flank to a depth of ~160 mbsl. At this depth, there is a break in slope that is thought to mark the old subaerial/ submarine boundary when the volcano's growth rate was equal to or greater than its subsidence rate [*see Moore and Campbell, 1987*]. If this is an old shoreline, then Mauna Loa has subsided at least 160 m. *Moore and Clague* [*1992*] identified a flat crest on the rift down to at least 500 mbsl and perhaps as deep as 750 mbsl, based on single-beam profiles across the rift. They used these depths and the average subsidence rate of the volcano (2.6 mm/yr) to suggest that there had been little volcanic activity along this portion of the rift during the last 170 to 270 ky. The coastal portion of the rift, however, underwent extensive volcanism until probably just before deposition of the Pahala Ash, which caps the lower rift zone and is at least 31 ka [*Lipman and Swenson, 1984*]. We saw no soil horizons separating any of the flows in the ~150-m-thick section we measured up the Kahuku Pali, so there probably were no significant time breaks in volcanic activity prior to deposition of the ash. Furthermore, we observed pillow lavas as shallow as 300 mbsl during dive 183. If our revised depth for the slope break is used (160 m), then the age when volcanic activity may have slowed relative to subsidence would be ~60 ka. The absence of the old shoreline terrace on the southwest side of Mauna Loa and the ruggedness of the landslide scar indicate that the landslide is young and probably <60 ka.

One surprising feature of the map is the paucity of cones along the ridge that is considered the axis of Mauna Loa's southwest rift zone [*Lipman and Swenson, 1984*]. This impression was confirmed by examining a 10 m contour map of the ridge and the videotapes taken during dive 185 along its crest. In contrast, cones are common in a 3-km-wide zone along the submarine portion of Kilauea's east rift zone [*Lonsdale, 1989; Clague et al., in press*]. One explanation for the scarcity of cones along Mauna Loa's submarine ridge is that it is not the axis of the southwest rift zone but instead a remnant of the east flank of the rift zone left behind by the east Ka Lae landslide. This interpretation is supported by the abundance of dikes that were observed in the submarine cliff face during our submersible dives and those of *Fornari et al.* [*1979*] and new magnetic data for the rift zone, which show that the axis of the magnetic dipole is offset to the west of the ridge near the base of the cliff [*Smith et al., in press*]. Along Kilauea's submarine east rift zone, the dipole is centered along the topographic axis of the rift zone [*Smith et al., in press*]. Therefore, the center of Mauna Loa's southwest rift zone has been displaced two to three kilometers west of the present topographic high (Figure 2). The westward shift in the axis of the submarine portion of the southwest rift would make the bend in the rift at about 700 m above sea level less severe and would not require an eastward offset near the upper end of the Kahuku Pali as previously thought [*Lipman and Swenson, 1984*].

PETROGRAPHY

The lavas from the submarine southwest rift zone vary dramatically in mineralogy (Table 1) ranging from weakly phyric (<2 vol.% phenocrysts) to extremely olivine phyric (~47 vol.%). Most of the samples from the cliff face contain only olivine phenocrysts. The other ~40% contain <1 to 4 vol.% small phenocrysts of plagioclase and augite, in addition to variable amounts of olivine. In contrast, all of the dive 185 samples contain rare to common plagioclase and augite phenocrysts (Table 1). Only a few of the dredge haul lavas contain only olivine phenocrysts; most also have plagioclase and augite phenocrysts [*Garcia et al., 1989*]. Among our suite of submarine Mauna Loa lavas, about 65% of these samples are olivine-rich (>10% olivine phenocrysts); 44% are picritic (>15 vol.% phenocrysts). The abundance of olivine in these submarine Mauna Loa lavas contrasts with previous studies of subaerial Mauna Loa lavas, which found that picrites constitute 7-11% of historical flows and ~15-20% of prehistoric flows [*Macdonald, 1949; Lockwood and Lipman, 1987*]. Hypersthene is common in subaerially erupted Mauna Loa lavas [*Macdonald, 1949*], but is rare in the submarine lavas.

About 90% of the olivine phenocrysts are undeformed euhedra. Some of these grains share crystal faces forming multicrystal aggregates, many with pockets of glass between crystals. Some euhedral grains with glass inclusions have weakly developed subgrain boundaries or kink bands. Traditionally, kink-banded olivines are thought to have been deformed in the solid state [*e.g., Raleigh, 1968*]. Glass inclusions, however, are unlikely to be preserved in such olivines. *Wilkinson and Hensel* [*1988*] suggested that olivine phenocrysts can be deformed in a magma during its ascent through narrow cracks. Some of the olivine-rich lavas contain <1 to 3 vol.% strongly deformed, anhedral grains and aggregates without glass inclusions. These olivines are probably xenocrysts or remnants of disaggregated xenoliths (see Table 1).

Spinel commonly occurs as inclusions in olivine, although it also is present as microphenocrysts in some of the more mafic samples. These more mafic samples contain both brown and opaque spinels. The other lavas contain only opaque spinel. Both types of spinel are always euhedral.

The plagioclase and pyroxene phenocrysts and microphenocrysts are generally subhedral to euhedral, although rare, round or ragged xenocrysts are present in some lavas. Many of the augites display hour-glass zoning; some have weak concentric zoning. The orthopyroxenes are unzoned optically and are somewhat elongate. The plagioclase crystals show no obvious petrographic signs of compositional zoning.

Lavas with obvious disequilibrium textures (e.g., resorbed grain boundaries, disrupted zoning, abundant inclusions) are identified as "mixed magmas" in Table 1. The olivine-rich lavas rarely show these features, but they are common among the samples collected along the ridge axis and from the dredge hauls.

GEOCHEMISTRY

Analytical Methods

Mineral and glass compositions were measured using the University of Hawaii, five-spectrometer Cameca SX-50 electron microprobe. Natural mineral and glass standards were used for calibration and a PAP- ZAF matrix correction

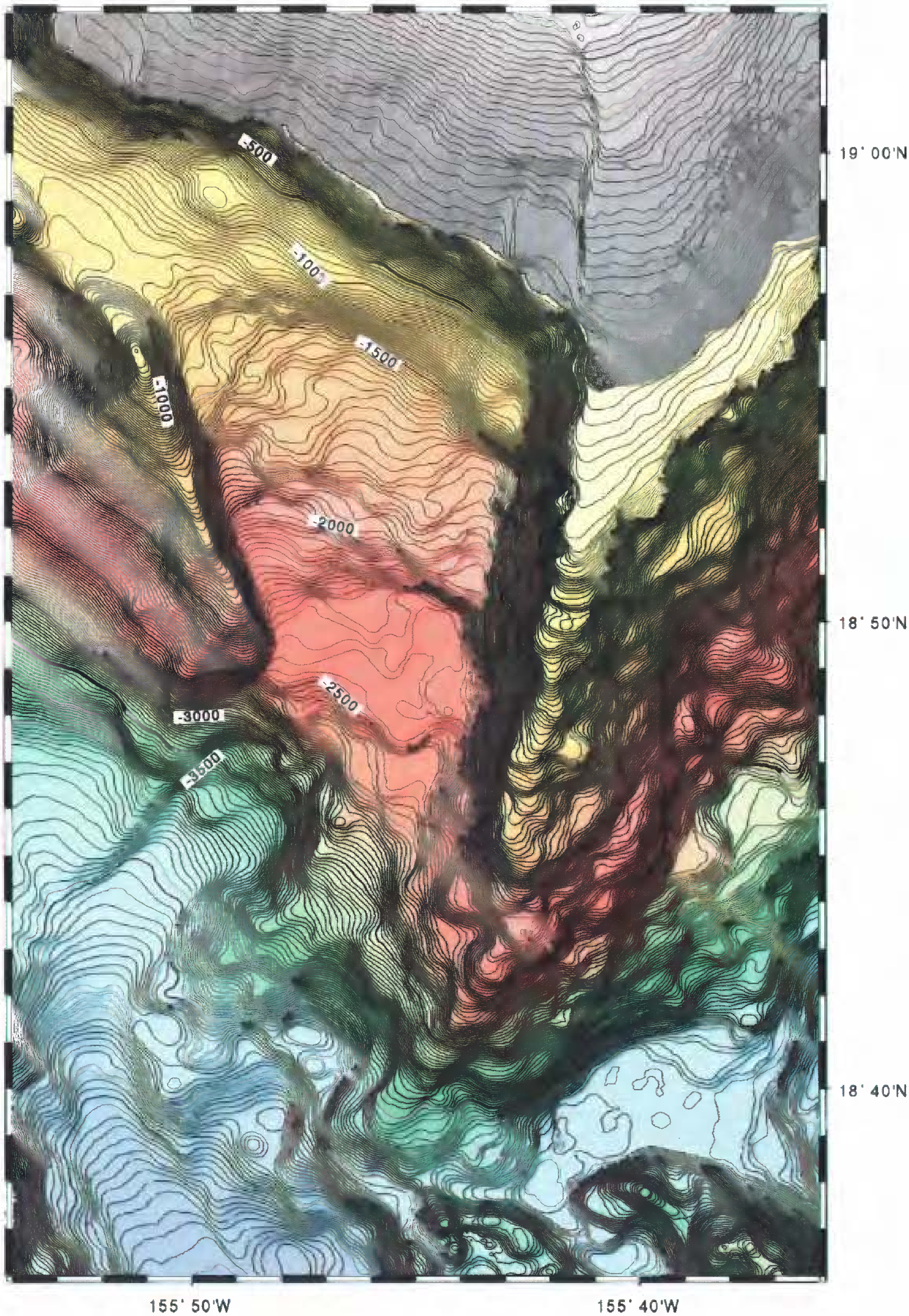

Plate 1. Shaded bathymetric map of the southwest rift zone of Mauna Loa. This map combines previous NOAA multibeam survey data from both sides of the rift with new multibeam data along the rift. The illumination angle is from the north and the contour interval is 20 m with every 500 m interval below sea level shown by a heavier line.

TABLE 1. Petrography[1] and Water Depth of Collection (mbsl) for Submersible Collected Lavas from Mauna Loa's Southwest Rift Zone

Sample	Depth Collected	Olivine		Plagioclase		Cpx		Opaques	Matrix	Glassy Margin	Mixed Magma; Comments
		ph	mph	ph	mph	ph	mph	mph			
182-1	1420	33.4	4.2	<0.1	0.2	0.6	0.2	0.2	61.2	No	No; oliv xenos
182-2	1405	11.8	7.6	0.6	0.6	-	0.6	0.2	78.6	No	No
182-3	1395	11.0	8.4	0.2	1.2	<0.1	1.4	<0.1	77.8	Yes	Mixed; gabbro clots
182-4	1375	33.0	22.2	-	-	-	2.4	0.2	42.2	No	No; oliv xenos
182-5	1335	1.8	1.6	-	<0.1	-	0.4	<0.1	96.2	Yes	No; oliv xenos
182-6	1310	30.0	20.4	-	-	-	-	0.2	49.4	Yes	No; oliv xenos
182-7	1265	44.0	20.4	-	-	-	-	0.2	35.4	Yes	No
182-8	1235	29.0	10.8	-	-	-	-	0.2	60.0	Yes	No; oliv xenos
183-1	1200	47.2	12.8	-	-	-	-	0.4	39.6	No	No; oliv xenos
183-2	1135	30.2	8.4	-	1.4	-	-	<0.2	59.0	No	No; oliv xenos
183-3	1100	28.2	5.6	-	-	-	-	<0.1	66.2	Yes	No; oliv xenos
183-4	1075	-	<0.1	-	2.4	-	<0.1	-	97.6	No	No
183-5	1030	20.4	5.2	-	-	-	<0.1	0.2	74.2	No	No
183-6	1015	8.2	3.0	-	2.0	-	<0.1	<0.1	86.8	No	No
183-7	960	10.2	4.0	-	0.6	-	-	<0.1	85.2	Yes	No; oliv xenos
183-8	920	21.1	4.4	-	-	-	-	<0.1	74.2	No	No; oliv xenos
183-9	875	0.6	0.2	0.2	0.8	<0.1	0.6	-	97.6	No	No; gabbro clots
183-10	830	4.6	1.4	0.4	0.4	0.2	0.2	-	92.8	No	No?; oliv xenos
183-11	790	13.4	6.6	-	<0.1	-	<0.1	<0.1	80.0	Yes	No; oliv xenos
183-12	750	11.6	8.0	-	-	-	-	<0.1	80.4	Yes	No; oliv xenos
183-13	695	13.6	6.8	0.2	2.4	-	1.4	<0.1	75.6	No	Mixed; oliv xenos
183-14	650	11.8	6.8	1.4	3.0	0.4	2.0	<0.1	74.6	Yes	Mixed
183-15	630	15.8	6.6	-	-	-	<0.1	<0.1	77.6	Yes	No; oliv xenos
184-1	1790	9.6	2.0	2.4	1.6	1.6	1.0	-	81.8	No	Mixed
184-2	1735	12.6	1.6	-	-	-	-	-	85.8	Yes	No; oliv xenos
184-3	1680	32	2.8	-	-	-	-	0.2	65.0	No	No; oliv xenos
184-4*	1610	1.2	<0.1	1.2	12.6	2.0	0.2	-	82.8	No	No
184-5	1535	18.8	3.0	-	0.4	-	-	0.4	77.4	Yes	No; oliv xenos
184-6	1425	21.0	1.0	-	-	-	-	-	78.0	Yes	No
184-7	1240	21.0	8.2	-	-	-	0.2	<0.1	70.6	No	No
184-8	1020	0.8	<0.1	0.6	1.4	1.0	2.0	-	94.6	Yes	No; gabbro clots
184-9	775	19.6	2.8	0.4	1.8	0.2	1.2	<0.1	74.0	Yes	Mixed
184-11	745	5.4	0.4	1.7	9.4	2.2	2.0	-	79	Yes	Mixed; gabbro clots
184-12	575	15.4	1.4	1.6	3.2	1.4	2.4	0.2	74.0	Yes	Mixed
184-13	550	15.2	5.2	2.6	5.6	1.8	4.0	-	75.6	No	Mixed
185-1	1825	6.6	3.0	<0.1	1.8	0.4	2.6	-	85.6	Yes	No?; gabbro clots
185-2	1795	5.6	2.8	0.6	1.2	<0.1	1.2	<0.1	88.6	Yes	Mixed
185-3	1735	10.0	4.6	0.6	0.8	0.2	2.0	<0.1	81.8	Yes	Mixed
185-4	1700	5.8	0.6	3.4	2.2	1.8	2.4	<0.1	83.8	Yes	Mixed
185-5	1670	9.6	1.6	2.0	2.4	2.4	1.6	<0.1	81	No	Mixed
185-6	1655	7.8	1.0	1.6	1.8	3.2	1.8	<0.1	82.6	Yes	Mixed; gabbro clots
185-7	1620	1.6	1.2	1.8	1.4	3.4	2.0	<0.1	82.6	Yes	Mixed; gabbro clots
185-8	1560	9.0	0.4	5.4	2.6	5.4	3.2	<0.1	74.2	No	No
185-9A	1565	15.2	2.8	2.8	2.0	4.4	2.2	<0.1	70.6	No	Mixed; oliv xenos
185-9B	1565	5.0	0.4	6.0	3.4	8.0	2.4	<0.1	74.8	No	Mixed
185-10	1515	4.6	1.2	0.6	1.0	1.6	0.6	<0.1	90.4	Yes	No

[1]Modes are based on 500 points counted/sample.
*Dike.

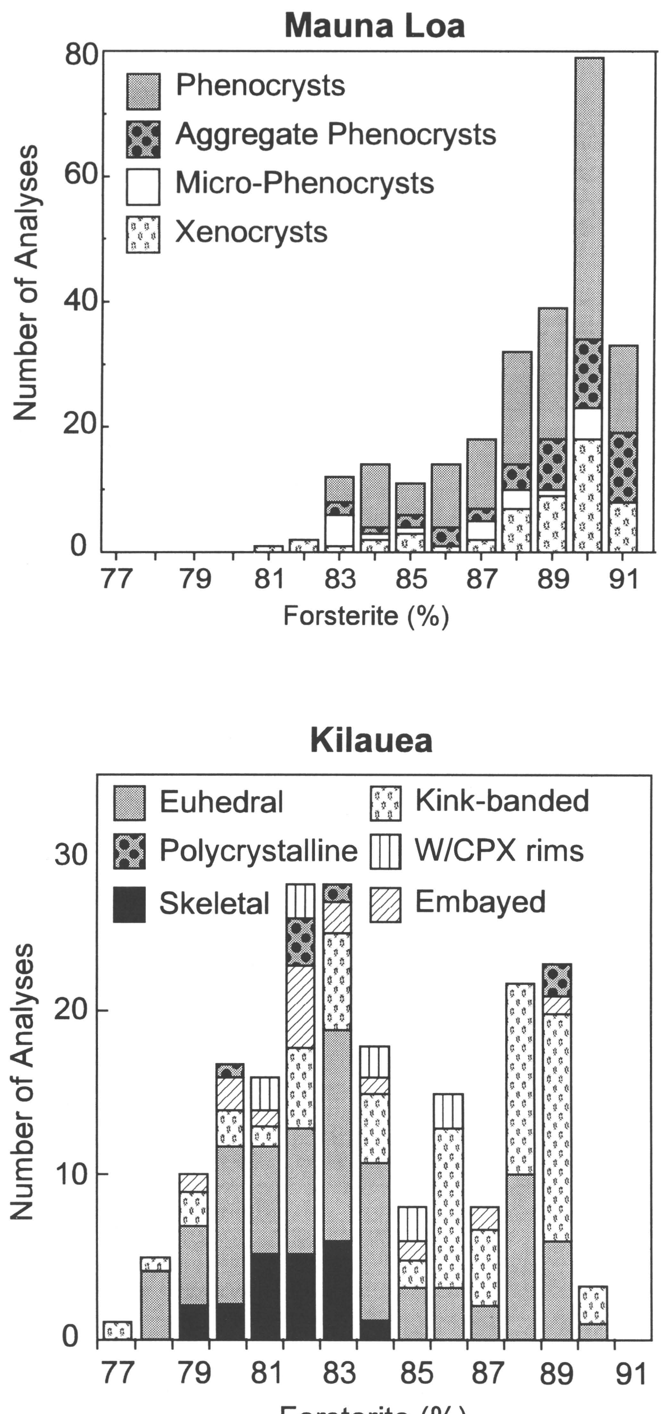

Fig. 4. Histogram of olivine core compositions (% forsterite) for submarine Mauna Loa lavas based on analysis of 255 crystals. Most of the grains contain high forsterite (89-91%). In contrast, Kilauea submarine lavas have lower average forsterite contents and more xenocrysts [*Clague and Denlinger, 1994*].

procedure was applied to all analyses. For olivines, spinels, and pyroxenes, a focused 20 nA beam was used; peak counting times were 40-80 s for major elements and 110 s for minor elements. A defocused (10 μm), 15 nA beam was used for plagioclase analyses. For glasses, a defocused (20 μm), 10 nA beam was used; counting times were 60 s, except for Na (40 s), S (300 s), K and P (100 s). Off-peak backgrounds were measured for half the peak counting times. The reported glass analyses are an average of 5 spot analyses; mineral analyses are an average of 3 spot analyses. Relative analytical error, based on repeated analysis of the Smithsonian standards A99 glass, hypersthene, Lake County plagioclase and San Carlos olivine, is <1% for major elements, <5% for minor elements and <2% for S in glass.

ICP-MS analyses of glass were made at Washington State University using methods described by *Garcia et al.* [*1993*]. About 100 mg of carefully hand-picked glass (i.e., free of minerals and alteration) were used for each analysis. For these analyses, accuracy and precision were <1 to 2 % for all elements based on repeat analyses of several samples including a Hawaiian basalt standard.

Mineral Chemistry

Olivine. Phenocrysts and microphenocrysts from representative lavas were analyzed to determine their compositions and zoning patterns (Table 2). They show a wide range of core compositions (82.0-91.3 Fo%) with no apparent correlation with crystal type (euhedral, undeformed

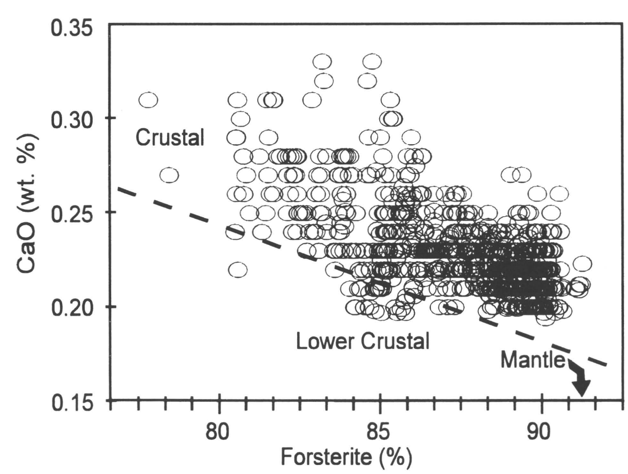

Fig. 5. CaO content (wt%) vs. percent forsterite in the cores of olivine phenocrysts. Note the modest increase in CaO content with decreasing Fo%, which is consistent with the experimental work of *Jurewicz and Watson* [*1988*]. All of the olivine is of crustal origin, based on their moderate CaO contents. The dashed line is an estimate of the boundary between olivines crystallized at upper and lower crustal depths. The highest forsterite crystals are of shallow origin.

vs. kinked; see Figure 4). Within individual lavas, the range may be small to large. Some of this variation may be an artifact of sectioning (see *Pearce, 1984*, for summary of this problem). Nevertheless, a histogram of the core compositions from the submarine lavas shows that they are forsterite-rich, with Fo 89-90 as the most common composition (Figure 4). In contrast, historically erupted Mauna Loa picrites have olivines with lower forsterite contents (87-89% Fo; *Wilkinson and Hensel, 1988; Rhodes, this volume*) and those from submarine Kilauea lavas have a bimodal variation with peaks at 82-83 and 88-89% Fo, with a strong preference for kink banding in the higher forsterite crystals (Figure 4).

The CaO contents of the Mauna Loa olivines are moderate and increase with decreasing forsterite content (Figure 5) as predicted from the experiments of *Jurewicz and Watson* [*1988*]. The CaO content in these olivines is consistent with equilibrium at shallow crustal pressures [*Stormer, 1973*].

The zoning in the olivines is normal in all analyzed grains (Figure 6) except for a few grains that have no apparent compositional zoning or modest reverse zoning (~1-2% Fo). The rare olivines with reverse zoning have lower forsterite contents (<84%). In contrast, about 20% of the olivine ana-

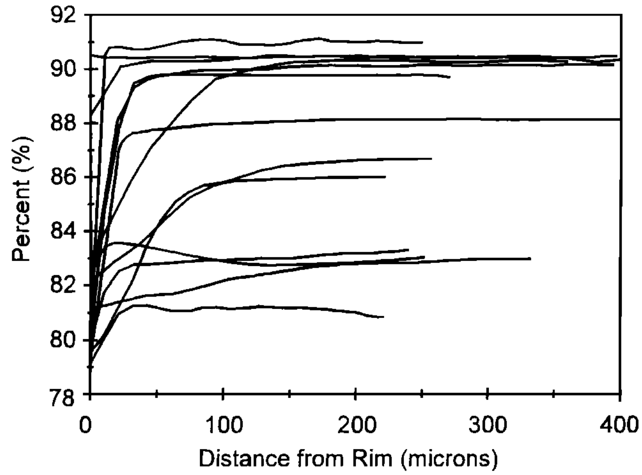

Fig. 6. Core to rim compositional zoning profiles for olivine phenocrysts from Mauna Loa submarine basalts. Note that all but one of the profiles show normal zoning with a narrow, strongly zoned rim. The crystals with wider rim zoning may have partially re-equilibrated in the magma or they may not have been sectioned through their core. One grain has no zoning and another has reverse zoning.

TABLE 2. Representative Microprobe Analyses of Olivine from Mauna Loa Submarine Lavas

Sample	SiO_2	MgO	CaO	FeO	NiO	Total	Fo
183-7	39.53	43.19	0.23	16.38	0.24	99.80	82.4
182-2	39.10	43.48	0.24	16.09	0.26	99.34	82.8
182-3	39.45	44.46	0.25	15.47	0.24	100.10	83.6
182-8	39.92	45.34	0.25	14.32	0.26	100.03	84.9
182-4	40.12	45.31	0.24	13.65	0.31	99.82	85.5
182-8	40.34	45.84	0.24	13.47	0.31	100.08	85.8
182-6	40.03	46.71	0.22	12.51	0.34	99.99	86.9
183-1	40.57	46.87	0.22	12.13	0.31	100.09	87.3
182-2	40.14	47.02	0.22	11.46	0.30	99.32	88.0
183-2	40.69	47.50	0.13	10.86	0.37	99.74	88.6
182-4	40.23	48.58	0.25	10.40	0.31	99.93	89.3
182-4	40.48	48.75	0.21	10.13	0.37	100.06	89.6
182-6	40.51	49.61	0.26	9.21	0.35	100.06	90.6
182-8	41.08	49.44	0.20	9.01	0.48	99.87	90.7
182-7	40.89	49.95	0.21	8.52	0.45	100.03	91.3
ML1-10	39.58	45.77	0.24	14.32	0.27	100.18	85.1
ML1-11	40.63	48.81	0.21	10.14	0.40	100.19	89.6
ML1-11*	39.07	43.30	0.25	17.60	0.18	100.50	81.4
ML2-3*	39.13	43.47	0.24	17.26	0.19	100.26	81.8
ML4-44	40.82	48.38	0.20	9.83	0.45	99.68	89.8

*Reversely zoned.

TABLE 3. Microprobe Analyses of Spinels from Mauna Loa Submarine Lavas

Sample	TiO_2	Al_2O_3	Cr_2O_3	FeO	MgO	Total	Fe_2O_3*	FeO*	Total	Mg#	Cr/Cr+Al	Host[x]
183-5	1.16	3.45	50.90	19.50	14.30	99.31	6.93	13.26	100.00	65.77	71.7	OL-90.0
183-5	1.57	3.90	43.85	28.40	10.45	98.17	10.13	19.28	99.18	49.13	67.9	OL-87.0
183-5	1.31	13.45	48.15	23.10	12.75	98.76	8.32	15.62	99.59	59.26	70.6	Matrix
182-3	1.26	14.75	49.50	19.70	14.05	99.26	6.43	13.92	99.90	64.28	69.2	OL-89.7
182-3	1.12	12.70	46.65	28.00	10.20	98.67	9.75	19.23	99.65	48.6	71.1	OL-83.6
182-3	1.22	4.80	46.15	24.40	12.05	98.62	8.47	16.78	99.47	56.14	67.6	OL-87.3
182-3	1.77	14.05	42.75	30.40	10.10	99.07	11.19	20.33	100.19	46.96	67.1	Matrix
183-11	1.10	13.87	49.25	19.75	13.90	97.87	7.03	13.43	98.57	64.85	70.4	OL-89.5
183-11	1.85	14.40	42.00	28.35	11.15	97.75	11.03	18.42	98.85	51.89	66.2	OL-83.2
183-11	1.85	13.10	49.78	23.65	11.50	99.88	5.97	18.28	100.48	52.85	71.8	Matrix
182-2	2.17	16.15	39.40	28.11	12.10	97.93	11.68	17.60	99.10	55.06	62.1	OL-85.3
182-2	1.03	14.10	49.40	19.15	13.95	97.63	6.57	13.24	98.29	65.25	70.1	OL-90.2
182-2	3.92	13.25	33.65	38.75	9.00	98.57	16.66	23.75	100.24	40.3	63.0	Matrix

[x]Host olivine forsterite content.
*Fe_2O_3 calculated assuming stoichiometry.

TABLE 4. Microprobe Analyses of Pyroxenes in Mauna Loa Submarine Lavas

Sample		SiO_2	TiO_2	Al_2O_3	Cr_2O_3	FeO	MnO	MgO	CaO	Na_2O	Total
182-2	core	52.75	0.61	2.79	--	6.48	0.17	17.78	18.9	0.23	99.71
	rim	54.09	0.52	1.68	--	6.24	0.17	18.80	17.86	0.22	99.58
182-3	core	52.15	1.12	2.65	--	7.98	0.15	16.48	19.19	0.32	100.04
	rim	52.31	0.85	3.30	--	6.97	0.19	17.86	18.0	0.23	99.71
183-14	core*	52.10	0.69	2.61	0.61	6.78	0.19	17.75	18.7	0.23	99.66
	core*	53.2	0.54	1.89	0.24	7.55	0.18	18.61	17.55	0.21	99.97
184-1	core	53.05	0.59	1.98	--	7.14	0.17	18.65	17.55	0.21	99.34
	rim	52.75	0.61	2.23	--	6.90	0.18	18.13	18.4	0.22	99.42
	core*	54.92	0.34	1.92	--	10.79	0.22	29.1	2.32	0.03	99.64
184-11	core	51.92	1.01	2.42	0.32	8.70	0.19	16.68	18.65	0.28	100.17
	rim	53.1	0.65	2.15	0.70	6.70	0.19	18.25	18.20	0.22	100.16
	core	54.4	0.65	1.5	0.11	14.2	0.28	26.95	2.20	0.04	100.33
	rim	54.7	0.50	1.9	0.38	12.4	0.25	27.5	2.8	0.04	100.47
185-3	core*	52.05	0.71	2.62	0.75	7.72	0.20	17.45	18.05	0.27	99.82
	core*	54.61	0.48	1.64	0.07	13.08	0.26	27.75	2.53	0.04	100.46
	core*	54.18	0.55	1.26	0.12	14.75	0.28	26.71	2.17	0.04	100.06

*Analyses with only cores are normally zoned or unzoned.

TABLE 5. Microprobe Analyses of Plagioclases in Mauna Loa Submarine Lavas

Sample		SiO_2	Al_2O_3	FeO	CaO	Na_2O	K_2O	Total	An%
182-2	core*	51.55	30.25	0.65	13.96	3.19	0.08	99.65	70.4
182-3	core*	49.02	32.33	0.60	15.81	2.35	0.06	100.17	78.5
	core	52.25	29.95	0.61	13.6	3.47	0.10	99.98	68.0
	rim	51.84	30.35	0.65	14.0	3.30	0.09	100.23	69.7
183-14	core	50.08	30.95	0.58	14.84	2.82	0.07	99.34	74.1
	rim	49.9	31.4	0.70	15.10	2.63	0.07	99.80	75.7
184-1	core	49.31	31.75	0.57	15.5	2.4	0.04	99.57	77.9
	rim	48.0	32.8	0.64	16.5	1.8	0.03	99.77	83.4
	core*	50.0	31.0	0.60	14.95	2.69	0.06	99.31	75.2
184-11	core	50.45	31.08	0.47	14.75	2.83	0.06	99.63	74.0
	rim	49.7	31.7	0.45	15.24	2.53	0.05	99.67	76.7
	core	50.81	31.06	0.58	14.65	2.86	0.06	100.02	73.6
183-3	core*	50.90	30.7	0.65	14.45	2.96	0.08	99.74	72.6
	core	52.95	29.3	0.77	12.67	3.92	0.15	99.76	63.5
	rim	52.22	29.7	0.72	13.24	3.48	0.13	99.49	67.2
ML1-10	core*	52.77	29.15	0.86	12.66	4.15	0.14	99.73	62.2
ML1-11	core*	52.49	27.28	1.59	12.07	4.44	0.11	99.48	59.6
ML2-3	core*	50.28	31.08	0.61	14.74	3.04	0.03	99.75	72.7
ML4-44	core*	52.05	29.67	0.53	13.69	3.59	0.07	99.60	67.5

*Analyses with only cores reported are normally zoned or unzoned.

lyzed from Kilauea submarine lavas have reverse zoning [*Clague et al., in press*].

Spinel. Microprobe analyses were made of spinel inclusions and microphenocrysts in four representative samples (Table 3). The microphenocryst and inclusion spinels are compositionally identical except in sample 182-2; its microphenocrysts have higher TiO2 and FeO contents (Table 3). The TiO2 content of the spinels is <4.0 wt%, and except for a few matrix spinels, usually <2 wt%. This is characteristic of magnesiochromites which crystallize in picritic magmas [*Wilkinson and Hensel, 1988*]. The Mg# and Cr/Cr+Al ratios of these spinels range from 40-66 and 62-77, which are identical to values obtained for spinels from Mauna Loa subaerial picrites [*Wilkinson and Hensel, 1988*] and Kilauea submarine olivine-rich basalts [*Clague et al., in press*]. The Mg# of the spinel inclusions correlates well with the forsterite content of the host olivine (Table 3). Titanomagnetite was found in the matrix of some of the more slowly cooled basalts.

Pyroxene. The clinopyroxenes in the submarine Mauna Loa lavas are augites with moderate to low Al, Ti, Cr, and Na contents (Table 4). The orthopyroxene are bronzites. The Mg# of the pyroxene cores range from 76-83 for the bronzites and 79-83 for the augites. Many of these pyroxenes are unzoned or have weak normal zoning, although reverse zoning is common in pyroxenes from some of the submarine lavas (e.g., 184-1).

There are few published pyroxene analyses for Mauna Loa lavas (i.e., a few grains from five historical flows; *BVSP, 1981; Rhodes, this volume*) to compare the data for the submarine lavas with. Our new pyroxene analyses are within the compositional range reported for these subaerial lavas, which are thought to have formed in low MgO, summit reservoir magmas [*Rhodes, this volume*].

Plagioclase. This mineral was analyzed in representative lavas from each dive and dredge haul. The anorthite content (An) of plagioclase in these submarine lavas ranges from 60-83, although most grains have An contents of 67-78 An (Table 5). This range overlaps and extends to higher An contents the few reported analyses of Mauna Loa lavas [*BVSP, 1981; Rhodes, this volume*] and those reported for submarine Kilauea lavas (64-76; *Clague et al., in press*). Many of the larger plagioclase crystals have modest reverse zoning (1-2% An), although some have greater variations (3-4% An). These reversals start 40 to 100 μm from the edge of the crystal and end 10 to 20 μm from the edge.

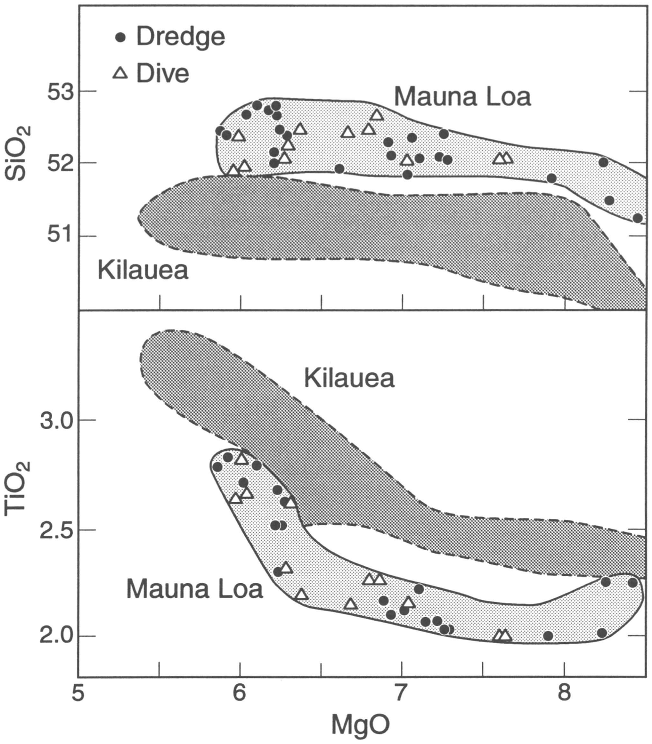

Fig. 7. MgO variation diagrams for TiO2 and SiO2 in glasses from Mauna Loa and Kilauea. The Mauna Loa glasses include dredged (Δ) and submersible-collected samples (●) The Kilauea field is based on submarine glasses [*Garcia et al., 1989*] and historically erupted subaerial glasses [*Garcia, unpublished*]. These elements and CaO are the best major element discriminants for separating lavas with MgO > 7 wt% from the two volcanoes [*Rhodes et al., 1989*].

Glass Chemistry

Major elements. Clear brown pillow-rim glasses were analyzed in this study to minimize the effects of mineral accumulation and thus obtain compositions more representative of Mauna Loa's magmas. Most of the dredge haul samples and about half of the dive samples have glassy margins [*Garcia et al., 1989* and Table 1]. These glasses were analyzed by microprobe for major and minor elements (including S). Two-thirds of the dive glasses were analyzed by ICP-MS for trace elements. The microprobe data for the dredge haul glasses were given in *Garcia et al.* [*1989*]. The microprobe data for the dive glasses are presented in Table 6. The submarine Mauna Loa glasses have a broad range in MgO content (5.8 to 8.3 wt%) and, like subaerial Mauna Loa lavas, have higher SiO2 and lower TiO2 contents at a given MgO content than glasses from its neighbor, Kilauea Volcano (Figure 7). The glasses from dive 185 have consistently lower MgO contents and more microlites of plagioclase and pyroxene than glasses from the other dives. The dive 185 lavas were probably erupted at lower temperatures than the lavas from the other dives (10° to 50°C based on the Mauna Loa empirical glass thermometer; *Monierth et al., this volume*).

The S contents of the glasses range from <0.01 to 0.101 wt%. There is a crude correlation of S content with depth for the dive glasses except for one sample (Figure 8). The dredged glasses overlap in S content with the deeper dive glasses. The S content of Hawaiian submarine glasses decreases sharply with depth of eruption above 1000 mbsl as a result of degassing [*Moore and Fabbi, 1971; Killingley and Muenow, 1975*]. All but two of our Mauna Loa glasses have low S contents for their depth of recovery compared to Kilauea glasses (Figure 8). The most likely explanation for their low S content is subsidence of the lavas after eruption. If the Mauna Loa lavas had S contents similar to those of Kilauea, then the section has subsided >400 m, with the deeper samples showing the most apparent subsidence. The subsidence interpretation is consistent with the bathymetry data, which indicate at least 160 m of subsidence of the old shore line, and with the discoveries along the southwest rift of rounded boulders at depths of 425 mbsl during dive 183 and at 450 mbsl by *Moore et al.* [*1990*].

Trace elements. ICP-MS analyses were made to determine trace element abundances (REE, Ba, Th, Nb, Y, Ta, Hf, U, Rb, Cs) in the dive glasses (Table 7). The most incompatible elements vary by a factor of ~2, with Th showing the most variation (217%). Plots of highly incompatible trace

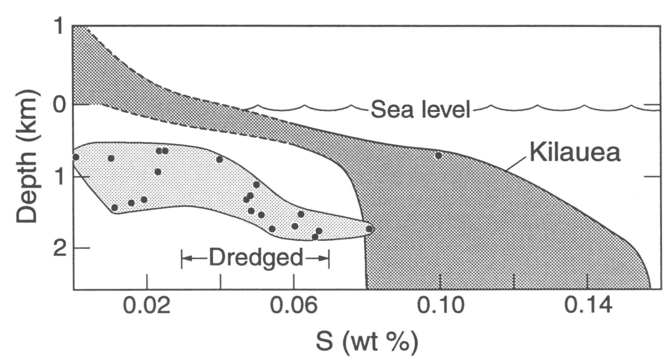

Fig. 8. S content vs. depth of sample collection (km below sea level) for glasses from submersible-collected and dredged lavas from Mauna Loa's southwest rift zone. The field for Kilauea glasses is shown for comparison [data from *Byers et al., 1985; Dixon et al., 1991; Muenow, unpubl.*]. At water depths <1 km, the S content of the Kilauea glasses decreases markedly because of degassing during eruption [*Moore and Fabbi, 1971; Killingley and Muenow, 1975*]. All but two of the Mauna Loa glasses have substantially lower S contents than predicted by the Kilauea field for their depth of collection. The low S content of the Mauna Loa glasses may be caused by subsidence of the rift zone.

TABLE 6. Microprobe Analyses of Glasses from Mauna Loa Southwest Rift Dives

Glass	SiO_2	TiO_2	Al_2O_3	FeO	MnO	MgO	CaO	Na_2O	K_2O	P_2O_5	S	Total	Mg#
182-3	52.25	2.18	14.04	10.56	0.17	6.88	11.15	2.27	0.32	0.18	0.016	100.02	53.7
182-4	52.15	2.05	14.13	9.90	0.15	7.25	11.10	2.33	0.30	0.19	0.020	99.57	56.6
182-6	51.50	2.17	13.45	10.35	0.16	8.25	10.75	2.21	0.31	0.19	0.049	99.39	58.7
182-7	51.26	2.17	13.41	10.53	0.16	8.42	10.70	2.16	0.31	0.19	0.049	99.36	58.8
183-3	52.03	2.01	13.45	10.30	0.20	8.24	10.46	2.10	0.31	0.19	0.051	99.34	58.8
183-7	52.08	2.11	13.94	10.20	0.17	7.25	10.93	2.21	0.33	0.19	0.023	99.43	55.9
183-11	52.35	2.09	14.07	10.04	0.16	7.08	10.95	2.30	0.30	0.18	0.015	99.54	55.7
183-12	52.45	2.04	14.16	9.95	0.18	7.29	10.88	2.22	0.31	0.14	0.001	99.62	56.6
183-14	51.95	2.48	13.80	10.69	0.17	6.65	10.82	2.37	0.38	0.20	0.026	99.54	52.6
183-15	52.05	2.24	13.98	9.90	0.18	7.13	11.10	2.20	0.37	0.20	0.025	99.38	56.2
184-2	51.81	2.01	13.73	10.49	0.16	7.90	10.90	2.18	0.30	0.18	0.082	99.74	57.3
184-5	52.06	2.11	14.01	10.20	0.16	6.95	11.22	2.29	0.32	0.20	0.063	99.58	54.8
184-8	52.01	2.54	13.60	11.78	0.18	6.26	10.30	2.23	0.40	0.23	0.012	99.54	48.7
184-9	51.91	2.12	13.99	10.42	0.15	7.01	11.11	2.21	0.31	0.20	0.040	99.47	54.5
184-11	52.19	2.32	13.66	10.68	0.18	6.24	10.63	2.43	0.38	0.18	0.101	98.99	51.0
185-1	52.67	2.71	13.57	11.46	0.17	6.20	10.03	2.49	0.44	0.27	0.066	100.08	49.1
185-2	52.40	2.85	13.55	11.53	0.19	5.91	9.88	2.54	0.50	0.28	0.067	99.70	47.7
185-3	52.45	2.80	13.62	11.50	0.19	5.84	9.71	2.52	0.50	0.34	0.054	99.52	47.5
185-4	52.35	2.70	13.88	11.25	0.17	6.23	10.22	2.39	0.51	0.29	0.061	100.05	49.7
185-6	52.43	2.61	13.89	10.81	0.15	6.29	9.95	2.41	0.47	0.32	--	99.33	50.9
185-7	52.50	2.51	13.71	11.46	0.18	6.22	9.89	2.47	0.38	0.22	0.063	99.60.	49.2
185-10	52.28	2.70	13.54	12.03	0.21	6.03	10.00	2.45	0.42	0.27	0.052	99.98	47.2
185-11	51.95	2.81	13.28	12.10	0.16	6.09	10.39	2.34	0.44	0.26	0.049	99.87	47.3

elements for the glasses from the dive-collected lavas and for whole-rock, XRF and INAA data for the dredge-collected lavas [*Gurriet, 1988*] define colinear trends (Figure 9). Plots of ratios of highly incompatible over moderately incompatible trace elements for the same glasses and lavas show broad linear and overlapping trends (Figure 10). Some of these ratios are greater than previously found for any subaerial Mauna Loa lava and overlap with ratios observed for Kilauea lavas (Figure 10).

DISCUSSION

Rock Type Variations: Spatial vs. Temporal Controls

Picritic basalts are rare in the volcanic record, especially among subalkaline lavas (<1%; *Wilkinson, 1986*). Geologic mapping of Hawaiian volcanoes has shown that picritic basalts are much more common on Hawaiian volcanoes (~5% for Kilauea; ~10-20% for Mauna Loa; *Macdonald, 1949*). Our current and previous studies of the submarine flanks of Hawaiian volcanoes [*Garcia et al., 1989*] indicate that picritic basalts are abundant on the flanks of these volcanoes (44-50%). The high temperature of the Hawaiian plume [*Sleep, 1990*] may be the cause of this greater abundance. Temperatures of >1550°C have been estimated for the Hawaiian plume [e.g., *Watson and McKenzie, 1991*], which would generate magmas with high MgO content.

A section along the subaerial portion of the Kahuku Pali

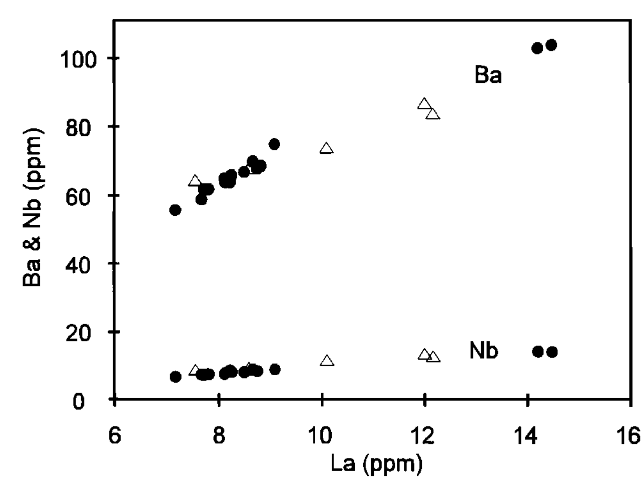

Fig. 9. Incompatible trace element variations for Mauna Loa submarine rift zone lavas. Symbols as in Figure 8. Data are from Table 5 for dive glasses and *Gurriet* [*1988*] for dredge whole-rocks. Note the collinear trend of the lavas and glasses.

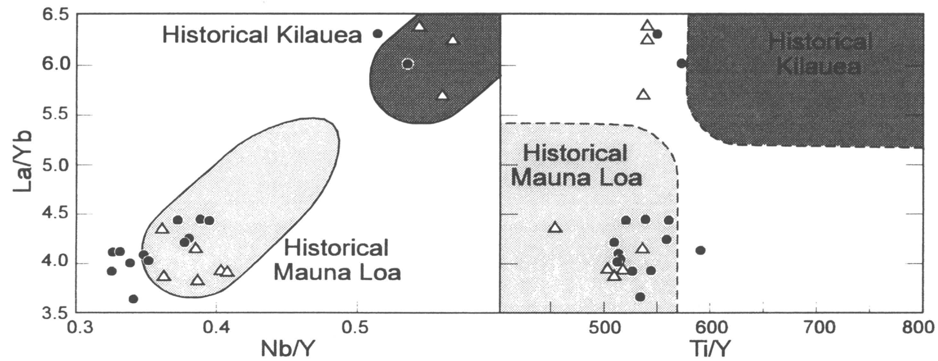

Fig. 10. Ratio-ratio plots for incompatible elements in Mauna Loa submarine rift zone lavas. The fields are for historical Mauna Loa [*Rhodes, unpublished*] and Kilauea lavas [*Garcia, unpublished*]. Although most of the submarine lavas plot in the Mauna Loa field for trace elements, five plot in the Kilauea field. These Kilauea-like lavas, however, have typical Mauna Loa Ti/Y ratios.

was measured to assist in our evaluation of the possible spatial and temporal controls on olivine abundance. This is one of the thickest subaerial sections on the volcano and the farthest from its summit (see Figure 3). We visually estimated the olivine content of the lavas and classified them into four broad categories: picritic (>15 vol.%), olivine-rich basalt (10-15 vol.%), olivine basalt (5-10 vol.%), and basalt (<5 vol.%). There is a clear temporal variation in this section. The upper third of the section is dominated by basalt (80%); the lower third of the section is mostly olivine-rich lavas (>95%; Figure 11). The same interpretation can be made for the submarine section of the rift. The samples from the ridge crest (dive 185) are younger than the lavas from the cliff sections. Only about one-third of the dive 185 lavas are olivine-rich compared to >80% for lavas from the other dives. Thus, there has been a substantial decrease in the abundance of olivine-rich lavas in the upper part of the two sections we examined on Mauna Loa's southwest rift. Nonetheless, the volcano is still occasionally erupting picritic basalts (e.g., 1852 and 1868 eruptions;). Unlike most of the submarine lavas, however, these subaerial lavas have lower forsterite content olivines (<89% Fo) and are interpreted to be cumulates flushed from shallow magma chambers [*Wilkinson and Hensel, 1988*].

The abundance of high forsterite olivines in the submarine lavas (Figure 4) indicates that they were derived from more mafic magmas, which avoided the buffering effects of evolved magma in the shallow summit magma chamber (3-7 km; *Decker et al., 1983; Rhodes, this volume*). The neutral buoyancy model of *Ryan* [*1987*] provides a good mechanism to allow the denser olivine-rich magmas to enter the rift zone without passing through the summit reservoir. The density of these olivine-rich magmas would have been much greater than expected for normal, subaerially erupted magmas (2.80 to 2.95 g/cm^3 vs. 2.65-2.70 g/cm^3; *Ryan, 1987*). The basics of a "magma density stratification" model are summarized in Figure 12. This model proposes that the distal portions of the rift zone are primarily supplied with olivine-rich magmas by deep dikes (7-10 km) that intrude along density contrast zones. The existence of deep dikes within Hawaiian volcanoes has been supported by recent geophysical work on Kilauea [*Delaney et al., 1990*]. Lower density, less MgO-rich magmas ascend into the shallow (2-6 km) reservoir system of the volcano and are primarily erupted subaerially.

The ability of Mauna Loa to maintain a deep conduit within its rift zones may depend on its magma supply rate. The dead coral reef and drowned paleo-shorelines on the south flank of Mauna Loa indicate that the volcano's growth rate has slowed relative to its subsidence rate [*Moore et al., 1990*]. Our age estimate for this slowdown (~60 ka) is consistent with the change in abundance of olivine in the upper part of the subaerial Kahuku and submarine sections.

Origin of Olivine-Rich Mauna Loa Submarine Lavas

Many of the olivine-rich lavas that we recovered from the submarine flanks of Mauna Loa are cumulates. This can be inferred from a plot of olivine forsterite content vs. whole-rock Mg# (Figure 13). On this plot, the lavas that have accumulated olivine plot below the equilibrium field. These lavas are strongly olivine-phyric (21-47 vol.%) and have very high MgO contents (19.4 to 32.8 wt%). A few low Mg# lavas have olivines that are too forsteritic for their bulk rock Mg#; these olivines may be xenocrysts or are early formed olivines that were not separated from the magma. Another group of lavas have olivines that plot within or near the equilibrium field. These may be the lavas most representative of parental magmas. These samples contain 11-16 vol.% olivine, have Mg# of 71.9-75.6 and MgO contents of ~13.3-17.4 wt%.

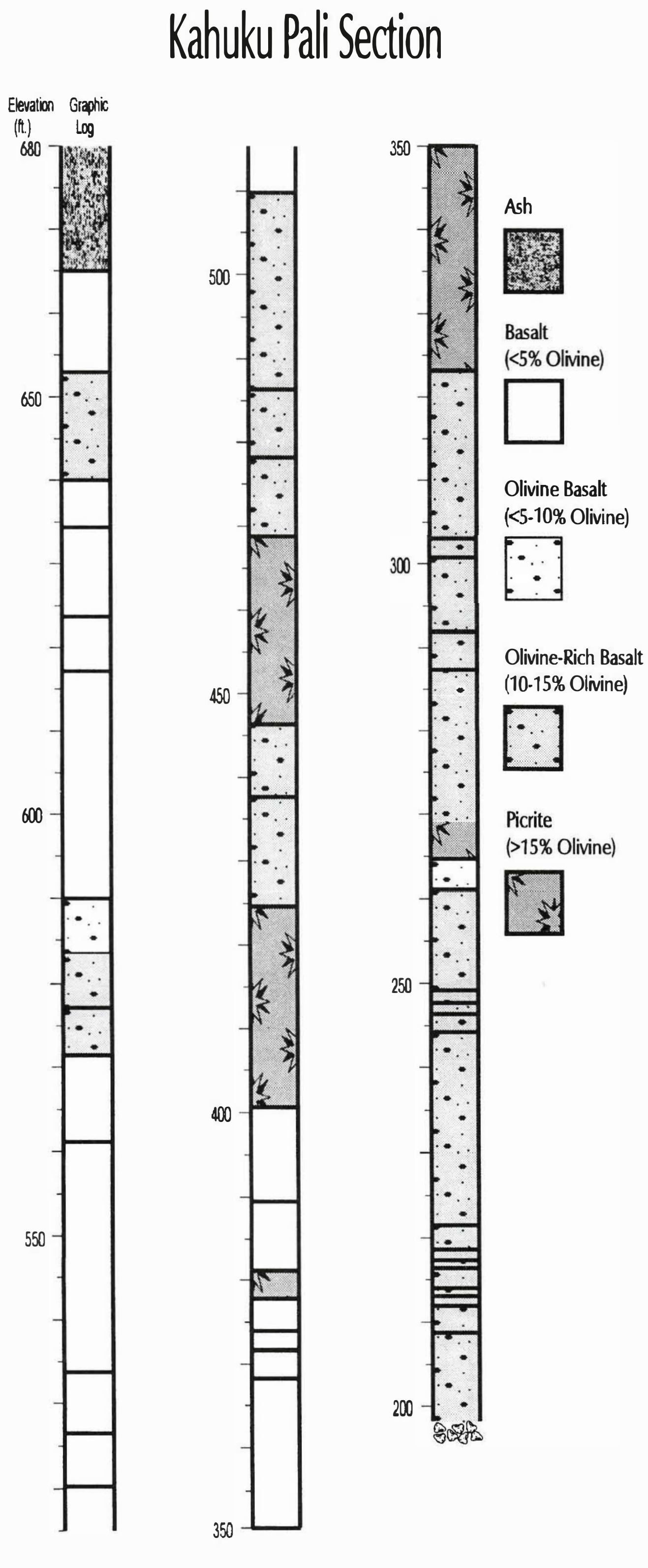

Some of the submarine lavas display petrographic (Table 1) and mineral compositional evidence (Table 6; Figure 6) of disequilibrium. Some of the minerals in these lavas are resorbed and have reverse zoning. The pyroxenes have low Mg# and must have grown in more evolved magmas than the coexisting olivines. If we assume a KD of 0.23 for Fe/Mg in augite/melt [*Grove and Bryan, 1983*], then the pyroxenes grew in magmas with Mg#s of 45 to 54; the olivine grew in magmas with Mg#s of 59 to 75 (Figure 13). These features are indicative of magma mixing involving olivine-rich and differentiated magmas. These differentiated magmas are similar to those erupted from the summit of Mauna Loa [e.g., *Rhodes, this volume*]. They may have been intruded from the summit reservoir through the shallower portions of the rift zone (2-4 km) and were mixed with the olivine-rich magmas from deeper dikes, or they may have been residual magmas from earlier intrusions that differentiated in the rift zone prior to mixing [c.f, *Wright and Fiske, 1971*]. Similar features were noted in, and explanations given for submarine lavas from Mauna Kea and Kilauea [*Yang et al., 1994; Clague et al., in press*]. Unlike lavas in those suites, our Mauna Loa suite includes lavas with no obvious signs of magma mixing (Table 1) and, therefore, they are more useful for inferring parental magma compositions.

Implications of Olivine-Rich Lavas for Mauna Loa Primary Magma Compositions

The MgO content of primary magmas for Hawaiian tholeiitic basalts has been a subject of considerable debate [see *Wilkinson and Hensel, 1988*, for a summary]. Estimates have ranged from 8 wt% [*Maaloe, 1979*] to 25 wt% [*Wright, 1984*]. A previous study of Mauna Loa subaerial lavas concluded that they were derived from parental magmas with 14-15 wt% MgO [*Wilkinson and Hensel, 1988*]. The discovery of glasses with up to 15 wt% MgO near the base of Kilauea [*Clague et al., 1991*] establishes a minimum parental magma MgO content and confirms that Hawaiian tholeiitic magmas are some of the most mafic magmas erupted during the Cenozoic.

The forsterite content of undeformed, euhedral olivine has frequently been used to infer the MgO content of the host magma [e.g., *Francis, 1985*]. This approach assumes equilibrium crystallization and that the early formed olivine is

Fig. 11. Stratigraphic section of the Kahuku Pali (lower, subaerial portion of Mauna Loa's southwest rift zone). Rock modes are based on hand specimen identification. The section is capped by the >31,000 year old Pahala Ash [*Rubin et al., 1987*]. The upper third of the section is dominated by basalts with variable amounts of small plagioclase phenocrysts. The lower third of the section consists of mostly olivine-rich basalts (>10 vol.% phenocrysts).

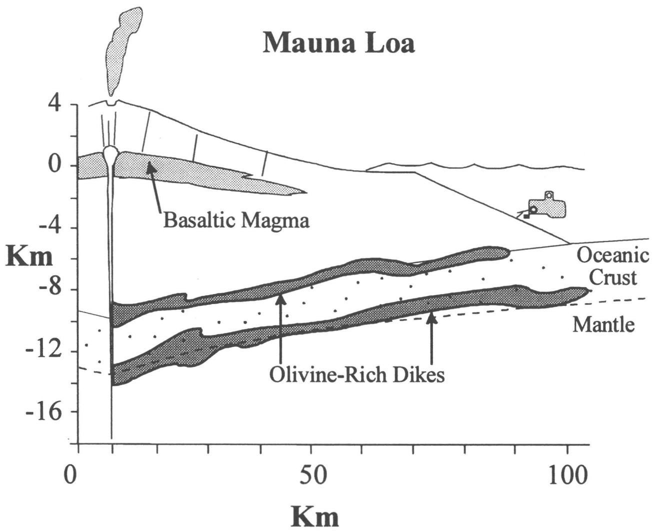

Fig. 12. Cartoon cross section of Mauna Loa illustrating the density stratification model for the volcano's magmatic plumbing system. The dense, olivine-rich magmas are intruded into the deeper portions of the rift zone at density contrast boundaries such as the Moho and are predominantly erupted from the distal portions of rift zones. Lower-density basaltic magmas rise into the upper part of the volcano's plumbing and are erupted preferentially on the subaerial parts of the volcano. Submersible not to scale.

carried with the ascending magma, a process that *Maaloe et al.* [*1988*] called "delayed fractionation". A correction for the effects of pressure on the olivine/melt partition coefficient [*Ulmer, 1989*] can be estimated from the olivine CaO content. Low CaO olivines form at higher pressure [*Stormer, 1973*], although the forsterite content of the olivine must also be considered [*Jurewicz and Watson, 1988*]. This approach generally yields host magmas with 12-15 wt% MgO because the olivines have <90% forsterite [*Wilkinson and Hensel, 1988; van Heerden and Le Roex, 1988*]. A recent study of Kilauea submarine olivine-rich basalts, however, found a Fo 90.7% olivine, which was related to a magma with 16.5 wt% MgO [*Clague et al., in press*].

Mauna Loa submarine basalts have olivines with the highest forsterite content ever reported for a Hawaiian tholeiitic basalt (91.3%). The moderate CaO contents of the olivines from these submarine lavas (0.18-0.31 wt%) indicate that an olivine/magma KD of 0.30 for FeO/MgO is appropriate. The calculated MgO content of the parental magma for the highest forsterite content olivine, assuming a ferrous iron content of 10% (based on measured values in Hawaiian lavas of 7 to 12%; e.g., *Byers et al., 1985*), would be ~17.5 wt% MgO. This Mauna Loa primary magma would have been most mafic and hottest (1415°C based on the empirical geothermometer for Mauna Loa tholeiites; *Montierth et al., this volume*) magma erupted during the Cenozoic.

If Hawaiian primary magmas have >16 wt% MgO, it would eliminate an apparent paradox between experimental studies on Hawaiian tholeiites that assumed a parental magma with only 16 wt% MgO and found no garnet [e.g., *Eggins, 1992*], and trace element studies that require garnet in the source for Hawaiian magmas [e.g., *Hofmann et al., 1984*]. *Eggins* [*1992*] predicted that experiments using parental magmas with MgO contents of 17 wt% or more would contain garnet as predicted by the REE studies.

Temporal Geochemical Variation

Mauna Loa lavas are known to be compositionally distinct from other Hawaiian volcanoes [e.g., *Rhodes et al., 1989*]. How long has this distinction persisted? *Wright* [*1971*] observed no difference in the major elements between historical and prehistoric Mauna Loa lavas. An attempt to test this interpretation using the oldest exposed subaerial

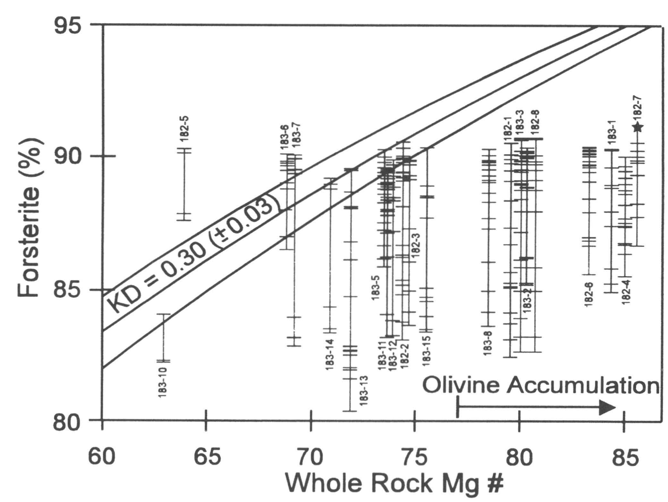

Fig. 13. Forsterite content of olivine cores vs. whole rock Mg# for 277 olivines from 21 submersible-collected lavas. The horizontal lines show the range of olivine core compositions for individual rocks (vertical lines). The equilibrium field is from *Roeder and Emslie* [*1970*] and *Ulmer* [*1989*] for lower pressure crystallization (<0.5 Gpa). Rocks with high Mg# (>76) have olivine forsterite contents too low to be in equilibrium with their whole rock Mg#; they have probably accumulated olivine. A few of the lavas have olivines with forsterite contents too high for their whole rock Mg#. They have either picked up xenocrysts or, more likely, not all of the early-formed olivine was separate from the magma prior to eruption. The lavas in the center of the figure with maximum olivine forsterite contents within the equilibrium field may be the most representative of near-primary compositions. The wide range in olivine composition within these lavas may be a consequence of delayed fractionation [c.f., *Maaloe et al., 1988*].

lavas from Mauna Loa (the Ninole basalts) yielded somewhat ambiguous results because these older lavas are altered [*Lipman et al., 1990*]. The submarine southwest rift zone lavas are unaltered and some must be even older lavas than the Ninole basalts. The major element contents of these lavas are identical to historical Mauna Loa lavas (Figure 7). Thus, there is no discernible difference in major element content in Mauna Loa lavas over the last several hundred thousand years.

Some studies of trace elements and isotopes in Mauna Loa lavas have suggested temporal variations in these ratios. *Budahn and Schmitt* [*1985*] and *Tilling et al.* [*1987*] noted lower incompatible element abundances in historical vs. prehistoric lavas at the same MgO content. *Kurz and Kammer* [*1991*] measured lower $^{3}He/^{4}He$ ratios in historic lavas, which are consistent with the trace elements. *Lipman et al.* [*1990*] and *Rhodes and Hart* [*this volume*], however, argue that alteration-resistant trace element and isotope ratio variations over the last 150 thousand years are not much greater than during historic times.

To extend this evaluation to older Mauna Loa lavas, we constructed a composite section for the submarine southwest rift dive lavas. The composite section sample depths (Table 7) were plotted against the Ba/Y in the glass, which displays a large but coherent variation relative to other trace element ratios. The section shows large variations over short intervals, especially for the ridge lavas, which are assumed to have been erupted during a limited time interval (Figure 14). Similar but smaller variations were observed for ratios of other incompatible elements (e.g., La/Yb). The Ba/Y variation in the section appears cyclic, which is similar to patterns observed in stratigraphic sections from other Hawaiian volcanoes (Koolau- *Frey et al., 1994;* Kahoolawe- *Leeman et al., 1994*). Significant variations in trace element and isotope ratios can occur over relatively short periods (<100 years for Mauna Loa; *Rhodes and Hart, this volume*; ~200 years for Kilauea; *Pietruszka and Garcia, 1993*). These variations are apparently related to source heterogeneity, since Pb and Sr isotopes display similar variations [*Pietruszka and Garcia, 1993; Leeman et al., 1994; Rhodes and Hart, this volume*]. The cause of these cyclic variations is problematic. Perhaps the source components have different solidus temperatures. Thus, during progressive melting, the proportions of the components in the melt vary as the low temperature component is consumed.

Five of the southwest rift lavas are geochemically distinct from all other analyzed Mauna Loa lavas. They have incompatible trace element ratios similar to the neighboring Kilauea volcano (Figure 10). These lavas also have lower $^{87}Sr/^{86}Sr$ ratios than subaerial Mauna Loa lavas (0.70359-0.70365 vs. 0.70368-0.70397; *Gurriet, 1988; Kurz and Kammer, 1991; Kurz et al., this volume*), which are within the range of typical Kilauea lavas (0.70347-0.70367; *Hofmann et al., 1984; Pietruszka and Garcia, 1993*). As mentioned above, however, the major element abundances of these samples have a Mauna Loa signature, especially for Ti (Figure 10), which is a good element for distinguishing Mauna Loa from Kilauea lavas [*Rhodes et al., 1989*]. Thus, separate processes control the major element contents and the trace element and isotope ratios. The major element contents are probably controlled by partial melting processes [e.g., *Watson and McKenzie, 1991*]. The trace element and isotope ratio variations require source heterogeneity. The absence of the Kilauea-like source component in subaerial Mauna Loa lavas is an indication that it has been exhausted, perhaps because it has a lower melting temperature than the other source components.

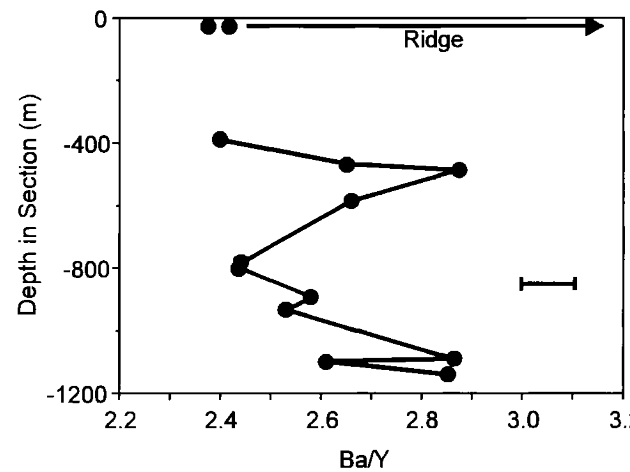

Fig. 14. Depth in section (table 7) vs. Ba/Y ratio for Mauna Loa submarine rift zone glasses. Note the large variations in the Ba/Y ratio over short depth intervals; this indicates rapid compositional changes in Mauna Loa magmas. The analytical error bar for the Ba/Y ratio is given in the lower right corner of the plot.

SUMMARY

A giant submarine landslide on the southwest flank of Mauna Loa provided the best available window into the magmatic history of this volcano. It created the deepest exposure into the volcano: a 1.3 km thick section into the interior of its southwest rift zone. A new bathymetric map, submersible observations and a new magnetic survey [*Smith et al., in press*] all indicate that the axis of the submarine portion of the southwest rift zone is two to three kilometers west of the topographic ridge, which was presumed to be the axis of the rift. The glassy pillow lavas collected from the submarine rift lavas are partially degassed, which may be explained by at least 400 m of subsidence. If the current

TABLE 7. ICP-MS Analyses of Glasses from Mauna Loa Southwest Rift Zone

Sample	Depth	La	Ce	Pr	Nd	Sm	Eu	Gd	Tb	Dy	Ho	Er	Tm	Yb	Lu	Ba	Th	Nb	Y	Hf	Ta	U	Rb
182-6	1140	8.25	20.5	3.16	15.4	4.22	1.50	4.64	0.74	4.35	0.83	2.22	0.33	1.87	0.26	66	0.57	8.4	23.1	2.96	0.53	0.18	5.0
182-7	1100	8.22	20.9	3.14	14.6	4.12	1.49	4.70	0.76	4.21	0.81	2.23	0.32	1.86	0.26	64	0.69	8.8	24.5	2.88	0.53	0.23	5.1
183-3	935	7.17	18.1	2.85	13.5	3.93	1.39	4.44	0.69	4.16	0.80	2.10	0.31	1.97	0.25	56	0.47	7.0	22.1	2.76	0.44	0.16	4.2
183-7	795	7.67	19.1	3.01	14.6	4.18	1.53	4.92	0.76	4.49	0.86	2.33	0.33	1.92	0.27	59	0.50	7.6	24.2	2.90	0.47	0.16	4.5
183-12	585	7.72	19.6	3.02	14.2	4.21	1.49	4.89	0.74	4.43	0.85	2.27	0.33	1.92	0.26	62	0.49	7.6	23.3	2.92	0.47	0.17	4.5
183-14	485	9.08	23.1	3.53	16.8	4.88	1.72	5.61	0.86	5.08	0.95	2.53	0.36	2.15	0.29	75	0.63	9.2	26.1	3.42	0.58	0.24	5.3
183-15	465	8.66	22.3	3.50	16.4	4.57	1.65	5.47	0.82	4.94	0.94	2.48	0.35	2.07	0.29	70	0.52	9.2	26.4	3.26	0.53	0.17	4.9
184-2	1090	8.11	20.4	3.11	14.8	3.98	1.43	4.53	0.69	4.22	0.79	2.08	0.30	1.84	0.25	65	0.56	7.8	22.7	2.93	0.50	0.18	5.0
184-5	895	7.81	19.9	3.05	14.7	4.29	1.15	4.94	0.75	4.52	0.88	2.33	0.35	1.92	0.27	62	0.52	7.7	24.0	3.07	0.48	0.17	4.9
184-6	785	8.13	20.7	3.16	14.8	4.50	1.56	5.01	0.76	4.70	0.92	2.45	0.35	1.98	0.28	64	0.55	8.0	26.2	3.15	0.51	0.18	4.5
184-8	390	8.82	22.5	3.52	17.1	4.92	1.17	5.57	0.86	5.14	0.99	2.67	0.39	2.26	0.31	68	0.59	-	28.3	3.62	-	0.20	5.4
185-1	10-25	14.47	34.4	4.90	21.9	5.58	1.92	6.27	0.93	5.57	1.04	2.71	0.39	2.30	0.32	104	1.02	14.3	30.0	4.09	0.89	0.31	8.0
185-3	10-25	14.20	33.5	4.82	21.9	5.65	1.92	6.08	0.92	5.55	1.05	2.80	0.40	2.37	0.32	103	1.01	14.3	28.9	4.20	0.87	0.30	7.9
185-7	10-25	8.49	22.3	3.53	16.6	4.82	1.71	5.38	0.83	5.05	0.96	2.55	0.37	2.17	0.31	67	0.51	8.3	27.7	3.34	0.52	0.17	4.8
185-11	10-25	8.74	22.4	3.44	16.6	4.82	1.71	5.41	0.83	5.21	1.00	2.54	0.37	2.13	0.32	68	0.58	8.6	28.6	3.55	0.54	0.19	5.1

*Depth is in meters for reconstructed composite submarine southwest rift zone section.

subsidence rate of the volcano (2.6 mm/yr; *Moore et al., 1990*) has not changed significantly in the last few hundred thousand years, then the lavas in this section were erupted between 150 to ~300 ka.

Olivine-rich basalts are extremely abundant among the submarine lavas from the rift zone (~65% contain >10 vol.% phenocrysts). Their abundance decreases dramatically in the upper part of the two southwest rift sections examined in this study and are much less common on the subaerial portion of the volcano (<20%). The decrease in abundance of olivine-rich basalts in the southwest rift sections may be related to a decrease in the volcano's magma supply rate during the last hundred thousand years. A magma density filter may operate within the volcano to control where olivine-rich basalts are erupted. This filter may force the dense, olivine-rich magmas to bypass the shallow summit reservoir of the volcano and to intrude into the deeper portions of the rift zones. Although many of these olivine-rich lavas are cumulates, they do contain high forsterite content olivine phenocrysts. These phenocrysts grew in high MgO magmas (up to 17.5 wt%). Thus, Hawaiian tholeiitic magmas are some of the most mafic and hottest magmas erupted during the Cenozoic.

Our results for these submarine Mauna Loa lavas indicate that there has been no apparent temporal change in major element characteristics over perhaps the last several hundred thousand years. There are, however, some submarine lavas with distinct trace element ratios that probably reflect a different source that is similar geochemically to that of neighboring Kilauea. Thus, although the conditions of melt extraction for the volcano may not have changed, the source has varied. The Kilauea-like source represents a minor component for exposed Mauna Loa lavas. If it was more common in earlier Mauna Loa lavas, it may be a lower melting component that has been nearly or completely exhausted during the formation of this giant volcano.

Acknowledgments. We would like to thank the Pisces V diving team from the Hawaii Undersea Research Lab led by Terry Kerby, the captain and crew of the R/V Kila, and our diving companions Pete Lipman and Mark Kurz for their efforts in our successful dives on Mauna Loa's southwest rift zone. The assistance of Jennifer Parker in sample preparation, Bill Chadwick for merging our bathymetic data with those from previous NOAA cruises, Terri Duennebier with preparation of the color map, John Smith for showing us his unpublished submarine magnetic data for Mauna Loa, Aaron Pietruszka with measuring the Kahuku Pali section, and the Estate of S.M. Damon and personnel at the Kahuku Ranch for access to the Kahuku Pali section is gratefully acknowledged. Reviews by Di Henderson, Dan Fornari, and Tom Wright substantially improved this paper. This research was supported by NSF-Ocean Sciences. This is SOEST contrib. no 3942.

REFERENCES

Bargar, K. E., and E. D. Jackson, Calculated volumes of individual shield volcanoes along the Hawaiian-Emperor Chain, *U. S. Geol. Surv. J. Res.*, 2, 545-550, 1974.

Basaltic Volcanism Study Project, Pergamon Press, New York, 1286 p., 1981.

Budahn, J. R., and R. A. Schmitt, Petrogenetic modeling of Hawaiian tholeiitic basalts. A geochemical approach, *Geochim. Cosmochim. Acta*, 49, 67-87, 1985.

Byers, C., M. Garcia, and D. Muenow, Volatiles in pillow rim glasses from Loihi and Kilauea volcanoes, Hawaii, *Geochim. Cosmochim. Acta*, 49, 1887-1896, 1985.

Chadwick, W. W., J. G. Moore, M. Garcia, and C. G. Fox, Bathymetry-topography of south Mauna Loa volcano, Hawaii, *U. S. Geol. Survey Misc. Field Invest. Map* MF-2233, 1993.

Clague, D., and R. P. Denlinger, Role of olivine cumulates in destabilizing the flanks of Hawaiian volcanoes, *Bull. Volcanol.*, 56, 425-434, 1994.

Clague, D., W. S. Weber, and J. E. Dixon, Picritic glasses from Hawaii, *Nature*, 353, 553-556, 1991.

Clague, D., J. G. Moore, J. E. Dixon, and W. B. Friesen, Petrology of submarine lavas from Kilauea's Puna Ridge, Hawaii, *J. Petrol.*, in press.

Decker, R. W., R. Y. Koyanagi, J. J. Dvorak, J. P. Lockwood, A. T. Okamura, K. M. Yamashita, and W. R. Tanigawa, Seismicity and surface deformation of Mauna Loa volcano, Hawaii, *Eos Trans. AGU*, 64, 545-547, 1983.

Delaney, P. T., R. S. Fiske, A. Miklius, A. T. Okamura, and M. K., Sako, Deep magma body beneath the summit and rift zones of Kilauea volcano, Hawaii, *Science*, 247, 1311-1316, 1990.

Dixon, J. E., D. Clague, and E. M. Stolper, Degassing history of water, sulfur, and carbon in submarine lavas from Kilauea volcano, Hawaii, *J. Geology*, 99, 371-394, 1991.

Eggins, S. M., Petrogenesis of Hawaiian tholeiites: 1. Phase equilibria constraints, Contrib. Mineral. Petrol., 110, 387-397, 1992.

Fornari, D. J., D. W. Peterson, J. P. Lockwood, A. Malahoff, and B. C. Heezen, Submarine extension of the southwest rift zone of Mauna Loa volcano, Hawaii: Visual observations from U.S. Navy Deep Submergence Vehicle DSV Sea Cliff, *Geol. Soc. Amer. Bull.*, 90, 435-443, 1979.

Fornari, D. J., J. P. Lockwood, P. W. Lipman, M. Rawson, and A. Malahoff, Submarine volcanic features west of Kealakekua Bay, Hawaii, *J. Volcanol. Geotherm. Res.*, 7, 323-337, 1980.

Francis, D., The Baffin Bay lavas and the value of picrites as analogues of primary magmas, *Contrib. Mineral. Petrol.*, 89, 144-154, 1985.

Frey, F., M. Garcia, and M. Roden, Geochemical characteristics of Koolau volcano: Implication of intershield geochemical differences among Hawaiian volcanoes, *Geochim. Cosmochim. Acta*, 58, 1441-1462, 1994.

Garcia, M., D. Muenow, K. Aggrey, and J. O'Neil, Major element, volatile and stable isotope geochemistry of Hawaiian submarine tholeiitic glasses, *J. Geophys. Res.*, 94, 10525-10538, 1989.

Garcia, M., B. Jorgenson, J. Mahoney, E. Ito, and T. Irving, Temporal geochemical evolution of the Loihi summit lavas: Results from ALVIN submersible dives, *J. Geophys. Res.*, 98, 537-550, 1993.

Grove, T. L. and W. B. Bryan, Fractionation of pyroxene-phyric MORB at low pressure: An experimental study, *Contrib. Mineral. Petrol.* 84, 293-309, 1983.

Gurriet, P. C., Geochemistry of Hawaiian dredged lavas, unpubl. M.S. thesis, 171 pp., M.I.T., Cambridge, Mass., 1988.

Hill, D. D., and J. J. Zucca, Geophysical constraints on the structure of Kilauea and Mauna Loa volcanoes, *U. S. Geol. Surv. Prof. Paper*, 1350, 903-917, 1987.

Hofmann, A. W., M. D. Feigenson, and I. Raczek, Case studies on the origin of basalt, III. Petrogenesis of the Mauna Ulu eruption, Kilauea 1969-1971, *Contrib. Mineral. Petrol.*, 88, 24-35, 1984.

Jurewicz, A., and E. B. Watson, Cations in olivine, Part 1, Calcium, Contrib. Mineral. Petrol., 99, 176-185, 1988.

Killingley, J. S., and D. W. Muenow, Volatiles in Hawaiian submarine basalts determined by dynamic high temperature mass spectrometry, *Geochim. Cosmochim. Acta*, 39, 1467-1473, 1975.

Kurz, M. D., and D. P. Kammer, Isotopic evolution of Mauna Loa volcano, *Earth Planet. Sci. Lett.*, 103, 257-269, 1991.

Leeman, W., D. Gerlach, M. Garcia, and H. West, Geochemical variation in lavas from Kahoolawe volcano, Hawaii, *Contrib. Min. Petrol.* 116, 62-77, 1994.

Lipman, P. W., The southwest rift zone of Mauna Loa: Implications for structural evolution of Hawaiian volcanoes, *Am. J. Sci.*, 280-A, 752-76, 1980.

Lipman, P.W., Growth of Mauna Loa during the last hndred thousand years, rates of lava accumulation verus gravitional subsidence, this volume.

Lipman P. W., and A. Swenson, Generalized geologic map of the southwest rift zone of Mauna Loa volcano, Hawaii, *U. S. Geological Survey Misc. Inves. Map* I-1312, scale 1:100,000, 1984.

Lipman, P. W., W. R. Normark, J. G. Moore, J. B. Wilson, and C. E. Gutmacher, The giant submarine Alika debris slide, Mauna Loa, Hawaii, *J. Geophys. Res.*, 93, 4279-4299, 1988.

Lipman, P. W., J. M. Rhodes, and M. A. Lanphere, The Ninole Basalt - implications for the structural evolution of Mauna Loa volcano, Hawaii, *Bull. Volcanol.*, 53, 1-19, 1990.

Lockwood, J. P., and P. W. Lipman, Holocene eruptive history of Mauna Loa volcano, *U.S. Geol. Survey Prof. Paper* 1350, pp. 509-535, 1987.

Lockwood, J. P., P. Lipman, L. Petersen, and F. Warshauer, Generalized ages of surface lava flows of Mauna Loa volcano, Hawaii, *U. S. Geol. Survey Misc. Invest. Map* I-1908, 1988.

Lonsdale, P., A geomorphological reconnaissance of the submarine part of the East Rift Zone of Kilauea volcano, Hawaii, *Bull. Volcanol.*, 51, 123-144, 1989.

Maaloe, S., Compositional range of primary tholeiitic magmas evaluated from major element trends, *Lithos*, 12, 59-72, 1979.

Maaloe, S., R. B. Pedersen, and D. James, Delayed fractionation of basaltic lavas, *Contrib. Mineral. Petrol.*, 98, 401-407, 1988.

Macdonald, G. A., Hawaiian petrographic province, *Geol. Soc. Am. Bull.*, 60, 1541-1596, 1949.

Monierth, C., A. D. Johnston, and K. V. Cashman, An empirical glass-composition-based geothermometer for Mauna Loa lavas, this volume.

Moore, J. G., Rate of palagonitization of submarine basalt adjacent to Hawaii, *U.S. Geol. Survey Prof. Paper* 550-D, D163-D171, 1966.

Moore, J. G., Subsidence of the Hawaiian Ridge, *U. S. Geol. Surv. Prof. Paper* 1350, 85-100, 1987.

Moore, J. G., and J. F. Campbell, Age of tilted reefs, Hawaii, *J. Geophys. Res.*, 92, 2641-2646, 1987.

Moore, J. G., and D. Clague, Coastal lava flows from Mauna Loa and Hulalai volcanoes, Kona, Hawaii, *Bull. Volcanol.*, 49, 752-764, 1987.

Moore, J. G., and D. Clague, Volcanic growth and evolution of the island of Hawaii, *Bull. Geol. Soc. Am.*, 104, 1471-1484, 1992.

Moore, J. G., and B. P. Fabbi, An estimate of the juvenile sulfur content of basalt, *Contrib. Min. Petrol.*, 33, 118-127, 1971.

Moore, J. G and W. W. Chadwick, Jr., Offshore geology of Mauna Loa and adjacent areas, Hawaii, this volume.

Moore, J. G., D. Clague, R. Holcomb, P. W. Lipman, W. Normark, and M. Torresan, Prodigious submarine landslides on the Hawaiian ridge, *J. Geophys. Res.*, 9, 17,465-17,484, 1989.

Moore, J. G., W. R. Normark, and B. J. Szabo, Reef growth and volcanism on the submarine southwest rift zone of Mauna Loa, Hawaii, *Bull. Volcanol.*, 52, 375-380, 1990.

Moore, J. G, W. B. Bryan, M. H. Beeson, and W. R. Normark, Giant blocks in the south Kona landslide, Hawaii, *Geology*, 23, 125-128, 1995.

Pearce, T. H., The analysis of zoning in magmatic crystals with emphasis on olivine, Contrib. Mineral. Petrol., 86, 149-54, 1984.

Pietruszka, A. J., and M. Garcia, Geochemical variations of historical summit lavas from Kilauea volcano, Hawaii: Evidence from Pb, Sr and Nd isotopes and trace elements, *Eos Trans. AGU*, 74, 642, 1993.

Raleigh, C. B., Mechanisms of plastic deformation of olivine, *J. Geophys. Res.*, 73, 5391-5406, 1968.

Rhodes, J. M., Homogeneity of lava flows: Chemical data for historic Mauna Loan eruptions, *J. Geophys. Res.*, 88, A869-79, 1983.

Rhodes, J. M., Geochemistry of the 1984 Mauna Loa eruption: Implications for magma storage and supply, *J. Geophys. Res.*, 93, 4453-4466, 1988.

Rhodes, J. M., The 1852 and 1868 Mauna Loa Picrite eruptions: Clues to parental magma compositions and the magmatic plumbing system, this volume.

Rhodes, J. M., and S. R. Hart, Episodic trace element and isotopic variations in historic Mauna Loa lavas: Implications for magma and plume dynamics, this volume.

Rhodes, J. M., K. Wenz, C. Neal, J. Sparks, and J. P. Lockwood, Geochemical evidence for invasion of Kilauea's plumbing system by Mauna Loa magma, *Nature*, 337, 257-60, 1989.

Roeder, P. L., and R. F. Emslie, Olivine-liquid equilibrium, *Contrib. Mineral. Petrol.*, 29, 275-289, 1970.

Rubin, M., L. K. Gargulinski, and J. P. McGeehin, Hawaii radiocarbon dates, *U. S. Geol. Survey Prof. Paper* 1350, pp. 213-242, 1987.

Ryan, M. P., Neutral buoyancy and the mechanical evolution of magmatic systems, *Geochem. Soc. Spec. Pub.* 1, 259-287, 1987.

Sleep, N. H., Hotspots and mantle plumes: Some phenomenology, *J. Geophys. Res.*, 95, 6715- 6736, 1990.

Smith, J. R, A. N. Shor, A. Malahoff, and M. E. Torresan, HAWAII MR1 sidescan reflectivity, Seabeam bathymetry, and magnetic anomalies on the submarine southeast flank of Hawaii Island, Hawaii Seafloor Atlas, Sheet 4, Hawaii Institute of Geophysics and Planetology, Honolulu, in press.

Stormer, J., Calcium zoning in olivine and its relationship to silica activity and pressure, *Geochim. Cosmochim. Acta*, 27, 1815-21, 1973.

Tilling, R. I., T. L. Wright, H. P. Millard, Jr., Trace-element chemistry of Kilauea and Mauna Loa lava in space and time: A reconnaissance, *U. S. Geol. Surv. Prof. Paper* 1350, 641-689, 1987.

Ulmer, P., The dependence of the Fe2+-Mg cation-partitioning between olivine and basaltic liquid on pressure, temperature and composition, *Contrib. Mineral. Petrol.*, 101, 261-73, 1989.

Van Heerden, L. A., and A.P. Le Roex, 1988, Petrogenesis of picrite and associated basalts from the southern mid-Atlantic ridge, *Contrib. Mineral. Petrol.*, 100, 47-60.

Watson, S., and D. McKenzie, Melt generation by plumes: A study of Hawaiian volcanism, *J. Petrol.*, 32, 501-537, 1991.

Wilkinson, J. F. G., Classification and average chemical compostion of common basalts and andesites, *J. Petrol.*, 27, 31-62, 1986.

Wilkinson, J. F. G., and H. D. Hensel, The petrology of some picrites from Mauna Loa and Kilauea volcanoes, Hawaii, *Contrib. Mineral. Petrol.*, 98, 326-345, 1988.

Wright, T. L., Chemistry of Kilauea and Mauna Loa lava in space and time, *U. S. Geol. Survey Prof. Paper* 735, 39 p., 1971.

Wright, T. L., Origin of Hawaiian Tholeiite: A Metasomatic Model, *J. Geophys. Res.*, 89, 3233- 3252, 1984.

Wright, T. L., and R. S. Fiske, Origin of the differentiated and hybrid lavas of Kilauea volcano, *J. Petrol.* 12, 1-65, 1971.

Yang, H.-J., F. A. Frey, M. Garcia, and D. Clague, Submarine lavas from Mauna Kea volcano, Hawaii: implications for Hawaiian shield stage processes, *J. Geophys. Res*, 99, 15,577-15,594, 1994

Michael O. Garcia and Thomas P. Hulsebosch, Hawaii Center for Volcanology, Geology and Geophysics Department, University of Hawaii, Honolulu, HI 96822

J. Michael Rhodes, Department of Geology and Geography, University of Massachusetts, Amherst, MA 01003